Evaluation of New Secondary Organic Aerosol Models for a Case Study in Mexico City

Katja Dzepina[1,2,3], Rainer M. Volkamer[2], Sasha Madronich[3], Pierre Tulet[1,3,4], Ingrid M. Ulbrich[1,2], Qi Zhang[5], Christopher D. Cappa[6], Paul J. Ziemann[7], and Jose L. Jimenez[1,2 *]

[1]Cooperative Institute for Research in the Environmental Sciences (CIRES), University of Colorado at Boulder, Boulder, CO
[2]Department of Chemistry and Biochemistry, University of Colorado at Boulder, Boulder, CO
[3]National Center for Atmospheric Research – Atmospheric Chemistry Division, Boulder, CO
[4]Meteo France / CNRM-GREI, Toulouse, France
[5]Atmospheric Sciences Research Center, University at Albany, SUNY, Albany, NY
[6]Department of Civil and Environmental Engineering, University of California at Davis, Davis, CA
[7]Air Pollution Research Center, University of California, Riverside, CA

* Corresponding author (email: jose.jimenez@colorado.edu)

Supplementary Information Section

Section SI-1: List of abbreviations

AMS	Aerodyne aerosol mass spectrometer
BBOA	Biomass burning organic aerosols
BG-SOA	Background SOA
DF	Dilution factor
DOAS	Differential optical absorption spectroscopy
FTIR	Fourier transform infrared spectroscopy
G model	Glyoxal SOA model; uses Volkamer et al. (2007a) parameterization
G-SOA	Glyoxal SOA
G-$SVOC_g$	Measured gas-phase glyoxal
GC-FID	Gas chromatography coupled to flame ionization detector
HOA	Hydrocarbon-like organic aerosols
IVOC	Intermediate volatility organic compound
LIF	Laser induced fluorescence
MCMA-2003	Mexico City Metropolitan Area 2003 field campaign
MILAGRO-2006	Megacity Initiative: Local and Global Research Observations 2006 field campaign
NR-PM_1	Non-refractory submicron particulate matter
NT model	Non-traditional SOA model; uses Robinson et al. (2007) parameterization
NT-P-S/IVOC	Primary emitted S/IVOC in non-traditional SOA model

NT-SOA	SOA formed in non-traditional SOA model
NT-P-SVOC	Primary emitted SVOC in non-traditional SOA model
NT-S-$SVOC_g$	Secondary gas-phase SVOC formed in non-traditional SOA model
NT-S-$SVOC_{g+p}$	Total semivolatile (i.e. condensable) material formed in non-traditional SOA model; NT-$SSVOC_{g+p}$ = NT-SOA + NT-$SSVOC_g$
OA	Organic aerosols
OOA	Oxygenated organic aerosols
OOA-I	Fresher OOA
OOA-II	More aged OOA
PBL	Planetary boundary layer
PMF	Positive matrix factorization
POA	Primary organic aerosols
P-S/IVOC	Primary emitted S/IVOC in non-traditional SOA model
Q-AMS	Quadrupole-based Aerodyne aerosol mass spectrometer
SOA	Secondary organic aerosols
S/IVOC	Semi-volatile and intermediate volatility organic compounds
SVOC	Semi-volatile organic compound
S/$IVOC_{i,j,g+p}$	Semivolatile material formed in NT model, where *i* is initial volatility bin, *j* is the oxidation generation of

	products from primary emitted S/IVOC, and *g* and *p* refers to gas- and particle-phase, respectively.
VOC	Volatile organic compound
T model	Traditional SOA model; uses only Koo et al. (2003) parameterization
T-SOA	SOA formed in traditional model
UMR	Unit mass resolution
UT model	Updated traditional SOA model; uses Koo et al. (2003) parameterization for all species except for high-yield aromatics for which Ng et al. (2007) parameterization is used
UT-PVOC	Secondary product VOC (PVOC) formed in updated traditional model
UT-SOA	SOA formed in updated traditional model
UT-$SVOC_g$	Secondary gas-phase SVOC formed in updated traditional model
UT-$SVOC_{g+p}$	Total semivolatile (i.e. condensable) material formed in updated traditional model; UT-$SVOC_{g+p}$ = UT-SOA + UT-$SVOC_g$

Section SI-2: Additional Support of PMF Results used in This Study

The HOA spectrum retrieved from PMF (shown in Figures SI-25a) is similar to those of hydrocarbons and has a low oxygen-to-carbon atomic ratio (O/C), and its time series correlates well with combustion tracers such as CO, NO_x, and EC, with ambient ratios (e.g. HOA/CO) consistent with those determined by other methods and studies (Zhang et al., 2005ab; Takegawa et al., 2006; Lanz et al., 2007, 2008; Ulbrich et al., 2008; Aiken et al., 2007, 2008a). For these reasons it is interpreted as a surrogate of urban POA. Note that sources such as meat cooking and plastic burning produce AMS spectra very similar to vehicle emissions (Mohr et al., 2008) and thus these and other reduced OA primary sources are likely grouped into HOA by factor analysis.

OOA spectra have high oxygen content and show similarities to chamber SOA spectra such as high *m/z* 44 and low signal at higher *m/z* (Figures SI-25b and SI-25c), and typically correlate with photochemical products such as O_3, O_x, glyoxal, and ammonium nitrate during periods dominated by SOA production (Zhang et al., 2005b; Volkamer et al., 2006; Aiken et al., 2008a; Herndon et al., 2008). OOA correlates strongly with the SOA estimated with up to four other independent methods (Kondo et al., 2007; Takegawa et al., 2006; Aiken et al., 2008b; Docherty et al., 2008). For these reasons OOA is interpreted as an SOA surrogate arising from urban precursors.

BBOA correlates well with biomass burning tracers, such as acetonitrile, levoglucosan, elemental potassium and satellite fire counts (Aiken et al., 2008ab). The case studies described here were characterized by low regional BB influence (from forest and agricultural fires), as described later in this section, and thus the contribution of regional BB to OOA should be very small. The emitted VOC and SOA formed from urban burning sources such as biofuel use and trash burning are accounted for properly in our analyses, since we use the measured VOC (from all sources) in the model. Primary OA from regional biomass burning (forest and agricultural fires) can be an important contributor to OA concentrations in Mexico City (Salcedo et al., 2006; Molina et al., 2007; Aiken et al., 2008b). During MCMA-2003 the regional BB influence was important during the last part of the campaign, from about April 23 to May 4, 2003 (Salcedo et al., 2006; Molina et al., 2007). Figure SI-26 shows the time series of several variables and tracers related to biomass burning. The OA concentration is approximately

121 constant (besides a strong diurnal cycle) during the first part of the campaign and then
122 steadily increases during the BB-influenced period, together with the AMS proxy for
123 levoglucosan ("excess" *m/z* 60; *m/z* 60 / OA) and consistent with results from PMF. Fine
124 K arises from both biomass burning and dust sources (Johnson et al., 2006; Querol et al.,
125 2008). The concentration of K is smallest at the very beginning of campaign and
126 increases significantly towards the end of the campaign. MODIS satellite fire counts (C.
127 Wiedinmyer, NCAR, pers. comm.) are consistent with these tracers and show very low
128 fire activity in the region around the MCMA from the beginning of April until the later
129 part of the month. Fire counts in all of Mexico also have a minimum in the period April
130 9-14.
131 BB tracers are low during the case study of April 9, 2003, as shown in Figure SI-
132 27. In particular fine K reaches the *lowest value of the field campaign* during our case
133 study, and *m/z* 60 does not show an enhancement that would be indicative of fire
134 influence. Fire counts in the MCMA and surrounding mountains are zero. The period
135 around our case study was cloudy, which could bias the fire counts low if the thermal
136 signal from a fire is blocked by a cloud. However clouds are also associated with rain and
137 reduced radiation and thus fires are less likely under clouds. We are only aware of one
138 study which has quantified this effect: Schroeder et al. (2008) reported that the
139 probability of fires below clouds in the Amazon was about 1/4-1/3 of the probability of
140 fires when clouds were absent, indicating that the potential bias of the MODIS fire counts
141 due to cloud presence is small. Taken together these pieces of evidence strongly
142 suggested that our case study was not affected by primary emissions from regional
143 biomass burning.
144 Zinc (Zn) from PIXE measurements is a tracer for industrial emissions in Mexico
145 City. Mass loadings of Zn follow a different pattern than the BB tracers (Johnson et al.,
146 2006), with a minimum during the weekend of the holy week holiday period (April 18-
147 20), consistent with an industrial source. April 9, 2003 shows the highest levels of Zn
148 during MCMA-2003 in the early morning sample (Figure 1d). However, Zn loadings fall
149 to a low value for 12-6 pm, indicating that the industrial emissions associated with high
150 Zn loadings in early morning were not present later in the day, and that the increase is
151 OOA was unrelated to the sources of Zn.

Finally, note that if some of the locally-formed SOA arises from precursors emitted from biomass burning sources (either urban or regional), it should be accounted for by our model. Grieshop et al. (2008) report on chamber aging experiments of wood smoke, and conclude that a traditional SOA model using the measured gas-phase species underpredicts the SOA formed in the aging of biomass burning emissions by a factor of 5. The main SOA precursors according to the traditional model are light aromatic and monoterpenes, which are also included in our model. Grieshop et al. (2008) conclude that the rest of the observed SOA arises from a NT-SOA mechanism, which should also be accounted for in our model since the S/IVOC volatility distribution of wood smoke is similar to that from engine exhaust (Lipsky and Robinson, 2006; Shrivastava et al., 2006).

Supplementary Information References

Alfarra, M.R.: Laboratory and Field Measurements of Organic Aerosols Using the Aerosol Mass Spectrometer; Ph.D. Thesis, University of Manchester Institute of Science and Technology, 2004.

Canagaratna, M.R., Jayne, J.T., Ghertner, D.A., Herndon, S., Shi, Q., Jimenez, J.L., Silva, P.J., Williams, P., Lanni, T., Drewnick, F., Demerjian, K.L., Kolb, C.E., and Worsnop, D.R.: Chase Studies of Particulate Emissions from in-use New York City Vehicles, Aerosol Sci. Tech., 38, 555–573, 2004.

Kondo, Y., Miyazaki, Y., Takegawa, N., et al.: Oxygenated and water-soluble organic aerosols in Tokyo, J. Geophys. Res., 112, D01203, doi: 10.1029/2006JD007056, 2007.

Lanz, V.A., Alfarra, M.R., Baltensperger, U., et al.: Source attribution of submicron organic aerosols during wintertime inversions by advanced factor analysis of aerosol mass spectra, Environ. Sci. Technol., 42, 214-220, 2008.

Querol, X., Pey, J., Minguillón, M.C., Pérez, N., Alastuey, A., Viana, M., Moreno, T., Bernabé, R.M., Blanco, S., Cárdenas, B., Vega, E., Sosa, G., Escalona, S., Ruiz, H., and Artíñano, B.: PM speciation and sources in Mexico during the MILAGRO-2006 Campaign, Atmos. Chem. Phys., 8, 111-128, 2008.

Schroeder, W., Csiszar, I., and Morisette, J.: Quantifying the impact of cloud obscuration on remote sensing of active fires in the Brazilian Amazon, Remote Sensing of Environment, 112, 456–470, 2008.

Takegawa, N., Miyakawa, T., Kondo, Y., et al.: Seasonal and Diurnal Variations of Submicron Organic Aerosols in Tokyo Observed using the Aerodyne Aerosol Mass Spectrometer (AMS), J. Geophys. Res., 111, D11206, doi:10.1029/2005JD006515, 2006.

188 **Table SI-1**: Speciation and assumptions of UT model (adapted from Koo et al., 2003 and Ng et al., 2007).

Lumped precursor species name	**Measured precursor species**	**k_{OH} (k_{O3}) (cm^3 $molec^{-1}$ s^{-1})**	**Stoichiometric SOA yield, α (dimensionless)**	**c^* (300 K) (µg m^{-3})**
One-product precursors				
AAR3	Methylcyclopentane Cyclohexane Methylcyclohexane C7-Cycloparaffins n-Heptane, Heptanes isomers n-Octane, Octane isomers n-Nonane, Nonane isomers	8.43×10^{-12}	0.004	1.35
AAR4	>C8-Cycloparaffins n-Decane, Decane isomers Undecane isomers >C12-isomers	1.23×10^{-11}	0.014	1.80
OLE1	Propene 1-Butene 1-Pentene, 1-Pentene isomers 1-Hexene isomers	3.16×10^{-11} (8.92×10^{-18})	0.002	0.90
OLE3	1,3-Butadiene 2-Pentene isomers 2-Hexene isomers Cyclopentene >=Cyclohexene	6.59×10^{-11} (1.21×10^{-16})	0.004	1.12
C7OL	Heptene isomers	6.34×10^{-11} (1.15×10^{-16})	0.013	1.35
C8OL	Octene isomers	6.34×10^{-11} (1.15×10^{-16})	0.035	1.58
C9OL	Nonene isomers	6.34×10^{-11} (1.15×10^{-16})	0.044	1. 58
PHEN	Phenol	1.63×10-11	0.031	1.35

Lumped precursor species name	Measured precursor species	k_{OH} (k_{O3}) (cm^3 $molec^{-1}$ s^{-1})	Stoichiometric SOA yield, α (dimensionless)	c^* (300 K) (μg m^{-3})
One-product precursors – cont.				
BALD	Benzaldehyde Aromatic aldehydes	1.15×10^{-11}	0.0008	1. 58
CRES	Cresols	4.1×10^{-11}	0.034	1.58
ISOP[1]	Isoprene	1.02×10^{-10} (1.28×10^{-17})	0.015	0
Two-products precursors				
TERP	Terpenes	5.37×10^{-11} (8.52×10^{-17})	High-NO_x P1: 0.038 High-NO_x P2: 0.326	3.35 143.2
ARO1[2]	i) Toluene ii) Ethylbenzene i-, n-Propylbenzene i-Butylbenzene o-, m-, p-Ethyltoluene Diethylbenzene isomers	i) 5.96×10^{-12} ii) 9.57×10^{-12};	High-NO_x P1: 0.058 High-NO_x P2: 0.113 Low-NO_x: 0.36	2.54 23.28 N/A
BENZ	Benzene	1.23×10^{-12}	High-NO_x P1: 0.072 High-NO_x P2: 0.888 Low-NO_x: 0.37	0.33 121.63 N/A
ARO2[2]	i) 1,2,3-, 1,2,4-, 1,3,5-Trimethylbenzene ii) m-xylene iii) p-xylene iv) Styrene v) Naphthalene Methylnaphthalene isomers Other naphthalenes	i) 4.32×10^{-11}; ii) 2.36×10^{-11}; iii) 1.43×10^{-11}; iv) 5.20×10^{-11}; v) 2.30×10^{-11}	High-NO_x P1: 0.031 High-NO_x P2: 0.09 Low-NO_x: 0.30	1.44 39.47 N/A

ΔH_{vap} for all SOA products, except low-NO_x SOA products, is 36 kJ mol^{-1} (Volkamer et al., 2006). Low-NO_x SOA products are considered non-volatile (c*=0).

[1]Isoprene aerosol yields are adopted from Kroll et al., 2005b.

[2]ARO1 and ARO2 are defined after original Koo et al. (2003) lumping as AAR5 + toluene, and AAR6 + AAR7, respectively.

Table SI-2: Assumptions of the NT model (Robinson et al., 2007).

Lumped S/IVOC	Lumped S/IVOC fraction of total (%)	ΔH_{vap} (kJ mol^{-1})	c^* (300 K) (µg m^{-3})
NT-P-S/IVOC$_{1,g+p}$	1.2	112	0.01
NT-P-S/IVOC$_{2,g+p}$	2.4	106	0.1
NT-P-S/IVOC$_{3,g+p}$	3.6	100	1
NT-P-S/IVOC$_{4,g+p}$	5.6	94	10
NT-P-S/IVOC$_{5,g+p}$	7.2	88	100
NT-P-S/IVOC$_{6,g+p}$	12	82	1000
NT-P-S/IVOC$_{7,g+p}$	16	76	10000
NT-P-S/IVOC$_{8,g+p}$	20	70	100000
NT-P-S/IVOC$_{9,g+p}$	32	64	1000000

All species are reacting only with $OH^{\cdot}$, with $k_{OH} = 4 \times 10^{-11}$ cm^3 molec^{-1} s^{-1}.

Table SI-3: Gas-particle distribution of primary emissions S/IVOC at different temperatures and OA concentrations.

T (ºC)	c_{OA} (µg m^{-3})	Gas-phase Fraction (%)	Gas-phase / particle-phase Ratio
20	10	87	6.7
20	1	93	13.3
20	0.1	96	24.0
0	10	79	3.8
0	1	87	6.7
0	0.1	92	11.5
-20	10	67	2.0
-20	1	77	3.3
-20	0.1	85	5.7

Supplementary Information Figure Captions

Figure SI-1: HOA and OOA results from custom principal component analysis method (CPCA; Zhang et al., 2005a) used in Volkamer et al. (2006) and from the PMF method used in this paper.

Figure SI-2: Size distributions of the selected AMS species during April 9, 2003 for the following time periods: 5 am – 8 am (red), 9 am – 12 pm (yellow), 12 pm – 3 pm (green), and 3 pm – 6 pm (blue).

Figure SI-3: Data used to calculate primary particle-phase emissions in NT model: temperature (Fig SI-3a), planetary boundary layer (PBL) height (Fig. SI-3b), ratio of the P-S/IVOC mass in gas vs. particle-phase according to the equilibrium calculation with the HOA concentration and temperature and the parameters from Robinson et al. (2007) (SI-6ac), and estimated HOA ("interpolated HOA") (Fig. SI-3d). Also shown in Figure SI-3d are calculated primary emissions per time bin (10 min) ΔHOA. Note that the first point in the ΔHOA time series (Fig. SI-3d) (1.69 μg m^{-3} $10min^{-1}$, or ~10% of the total ΔHOA) is to account for the P-S/IVOC in equilibrium with the HOA already present at that point when our simulation starts. The variations in ΔHOA are coming from point-to-point variations in PBL height.

Figure SI-4: Comparison of the relative time dependence of measured AMS OOA and six different variants of the T and UT models also shown in Fig. 4. The model SOA is multiplied by a different factor in each case in order to allow the evaluation of the relative time dependence.

Figure SI-5: Parameters related to the calculation of the low- and high-NO_x branching ratio for the UT model. Panel (a): measured NO concentration. Panel (b): measured HO_2 ·

222

223

224

225 **Figure SI-6**: Concentrations of lumped model species for UT-SOA (Fig. SI-6a), UT-
226 $SVOC_g$ (Fig. SI-6b) and UT-PVOC (Fig. SI-6c) at 2 pm during our case study.

227 **Figure SI-7**: Comparison of measured OOA and model SOA for selected runs of T
228 model (T_3-SOA and UT_1-SOA) for four other days of MCMA-2003. Also shown are the
229 T_3-SOA and UT_1-SOA results for April 9, 2003 simulations (Fig. 4 of main text).

230 **Figure SI-8**: Concentrations of lumped species from the NT model at 2 pm during our
231 case study. The upper three panels show NT-SOA and the lower three panels show NT-S-
232 $SVOC_g$. The secondary NT-SOA (pink) and NT-S-$SVOC_g$ (blue) are stacked on top of
233 the primary model species NT-POA (gray) and NT-P-S/$IVOC_g$ (dashed gray). Since the
234 distribution of these species is really two-dimensional, we have lumped them in three
235 different ways for one-dimensional representation: the left panels lump the species by the
236 number of oxidation steps undergone, the middle panels by the current saturation
237 concentration of the species, and the right panels by the initial lumped bin of the species
238 (which is directly related to the initial saturation concentration).

239 **Figure SI-9**: Left: evolution of gas- and particle-phase species during April 10, 2003.
240 Right: total model species compared to measured species for April 10, 2003.

241 **Figure SI-10**: Left: evolution of gas- and particle-phase species during April 13, 2003.
242 Right: total model species compared to measured species for April 13, 2003.

243 **Figure SI-11**: Changes in speciation of model SOA and gas-phase species due to
244 evaporation and condensation under equilibrium ("model thermal denuder") for 2 pm

species in our case study. Fig. SI-11a and b: UT model species. Fig. SI-11c and d: NT model species binned by current volatility.

Figure SI-12: Results of kinetic evaporation calculation for model thermal denuder when evaporation coefficient is decreased from 1 (base-case) to 0.1, 0.01 and 0.001. Each panel compares the model base-case equilibrium (Fig. 10a) and kinetic (Fig. 10b) calculations to the kinetic calculations with evaporation coefficients 0.1, 0.01 and 0.001. Fig. SI-12a: NT model POA; Fig. SI-12b: total model SOA; Fig. SI-12c: NT model SOA; Fig. SI-12d: UT model SOA.

Figure SI-13: Results of kinetic evaporation calculation for model thermal denuder. Left: results when ΔH_{vap} of UT model is changed to 100 kJ mol^{-1}. Right: results when ΔH_{vap} of NT model is changed to 36 kJ mol^{-1}.

Figure SI-14: Results of kinetic calculation for model thermal denuder for different residence times: 3s (left) and 22s (right).

Figure SI-15: Results of kinetic evaporation calculations with evaporation coefficient = 1 for changing particle size for ± 200 nm. Fig. SI-15a: NT model POA; Fig. SI-15b: total model SOA; Fig. SI-15c: NT model SOA; Fig. SI-15d: UT model SOA.

Figure SI-16: Results of kinetic evaporation calculations with evaporation coefficient = 0.1 for changing particle size for ± 200 nm. Fig. SI-16a: NT model POA; Fig. SI-16b: total model SOA; Fig. SI-16c: NT model SOA; Fig. SI-16d: UT model SOA.

Figure SI-17: Changes in model species upon dilution for species present at 2 pm during our case study. Fig. SI-17a and b: UT model species. Fig. SI-17c and d: NT model species binned by current volatility.

Figure SI-18: Results of alternative dilution case study when the background SOA concentration is zero.

Figure SI-19: Results of alternative dilution case study when the background SOA concentration is 1 $\mu g\ m^{-3}$.

Figure SI-20: Changes in model species upon aging without dilution, starting with the speciation at the end of our case study at 2 pm. Left panels: UT model species. Right panels: NT model species binned by current volatility.

Figure SI-21: Results of sensitivity studies of the NT model when different amounts of IVOC are specified. Upper panels: SVOC : IVOC = 1 : 1 (left: SOA; right: gas-phase species). Middle panels: SVOC : IVOC = 1 : 3. Bottom panels: SVOC : IVOC = 1 : 1.5 (base case).

Figure SI-22: Model SOA base case results with the updated NT model parameters (Grieshop et al., 2008).

Figure SI-23: Volatility of each model SOA as well as total model SOA in kinetic calculation for the updated NT model parameters (Grieshop et al., 2008).

Figure SI-24: Atomic O/C ratios for model SOA species with the updated NT model parameters (Grieshop et al., 2008).

Figure SI-25: Comparison of spectra from PMF output and characteristic spectra from the AMS spectral database (Ulbrich et al., 2008). Fig. SI-25a: AMS database spectrum of diesel exhaust (Canagaratna et al., 2004) vs. HOA spectrum from our case study. Fig. SI-25b: AMS database spectrum of fulvic acid (Alfarra, 2004) vs. OOA-I spectrum from our case study. Fig. SI-25c: AMS spectrum of SOA from toluene photooxidation (Aiken et al., 2008a) vs. OOA-II spectrum from our case study.

Figure SI-26: (a) Time series for all of the MCMA-2003 campaign for the following variables: AMS total OA, AMS proxy for levoglucosan ("excess *m/z* 60", m*/z* 60 / OA), MODIS satellite daily fire counts in the region encompassing the MCMA and the surrounding mountains and all of Mexico, and PIXE elemental potassium (K) and zinc (Zn) from two impactor stages that capture particles in the size range 70-1150 nm.

Figure SI-27: (a) Time series during the period of April 9, 2003 case study for the following variables: AMS total OA, AMS proxy for levoglucosan ("excess *m/z* 60", m*/z* 60 / OA), MODIS satellite daily fire counts in the region encompassing the MCMA and the surrounding mountains and all of Mexico, and PIXE elemental potassium (K) and zinc (Zn) from two impactor stages that capture particles in the size range 70-1150 nm.

Figure SI-1

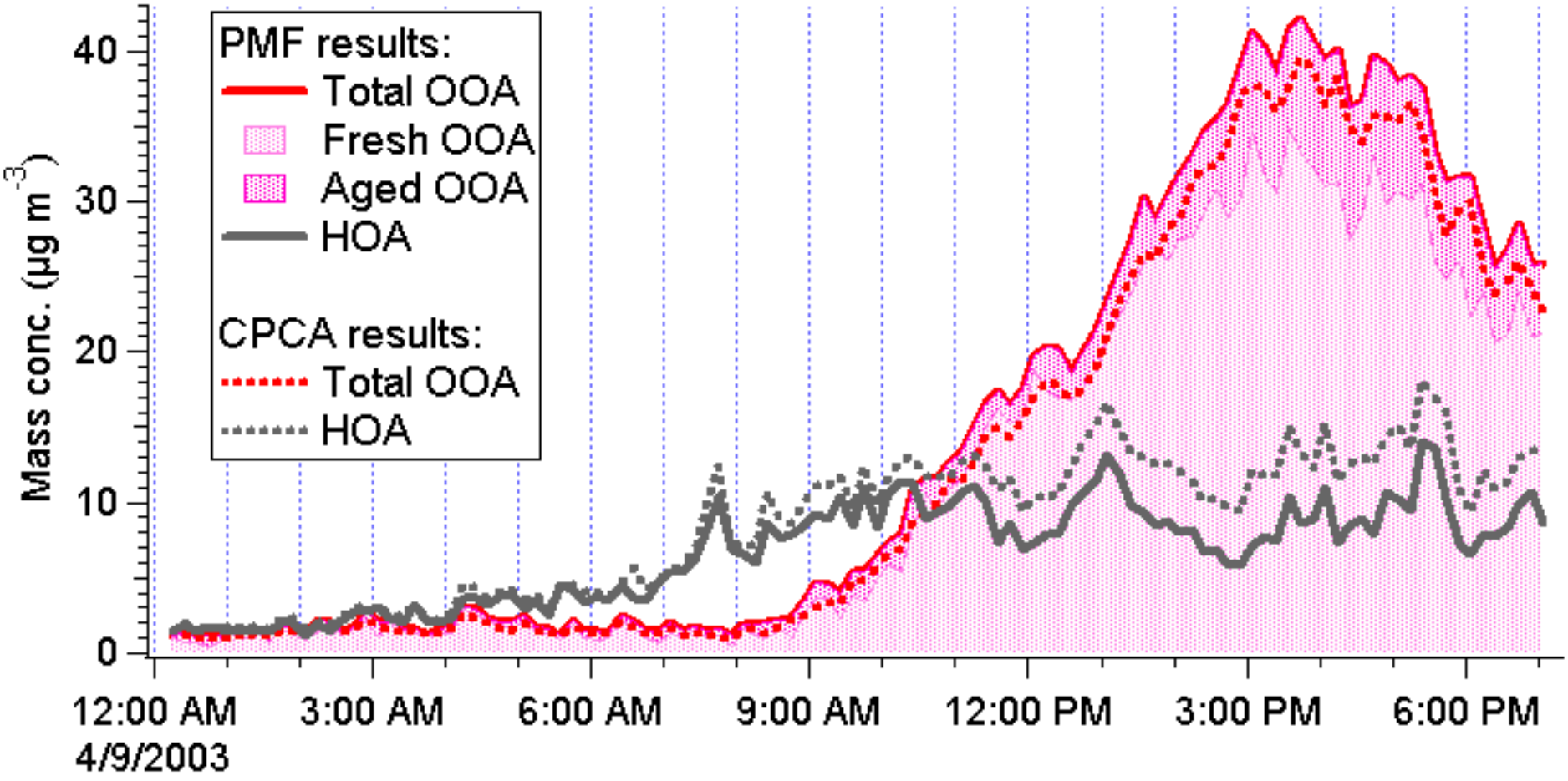
PMF results:
Total OOA
Fresh OOA
Aged OOA
HOA
CPCA results:
Total OOA
HOA
Mass conc. (µg m-3)
0
10
20
30
40
12:00 AM
4/9/2003
3:00 AM
6:00 AM
9:00 AM
12:00 PM
3:00 PM
6:00 PM

Figure SI-2

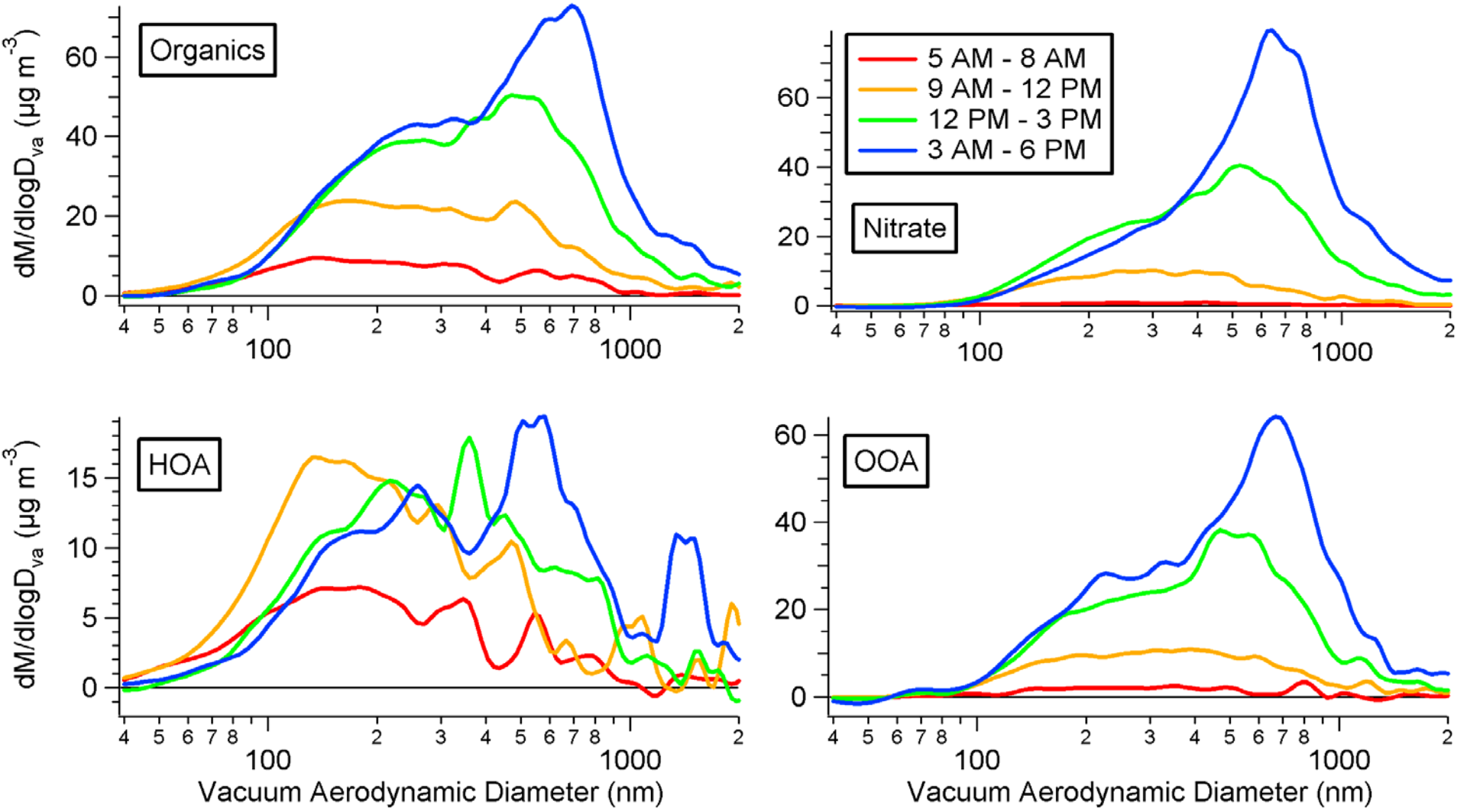
Organics
Nitrate
HOA
OOA
5 AM - 8 AM
9 AM - 12 PM
12 PM - 3 PM
3 AM - 6 PM
dM/dlogD$_{va}$ (µg m^{-3})
Vacuum Aerodynamic Diameter (nm)

Figure SI-3

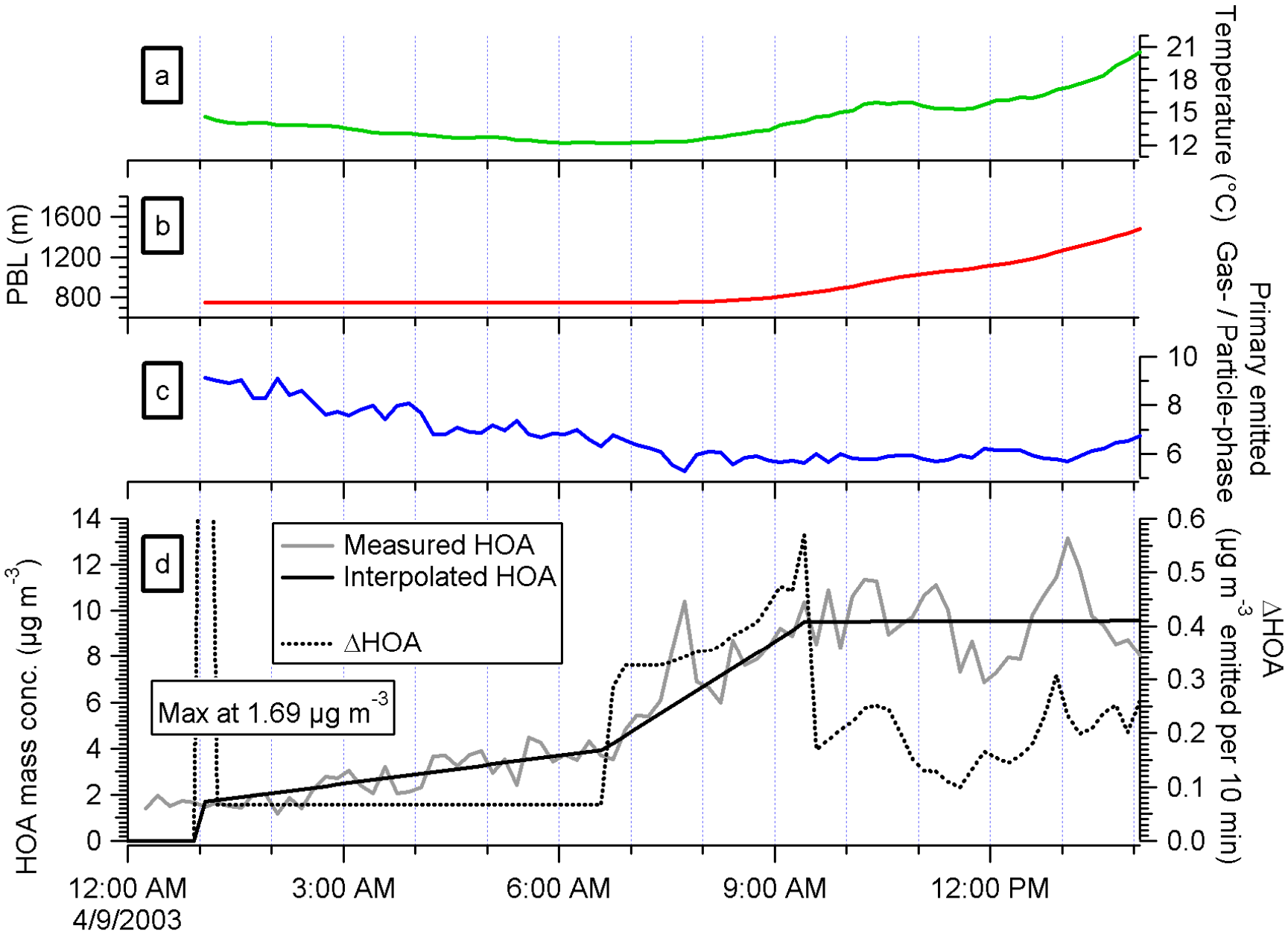
a
b
c
d
Temperature (°C)
21
18
15
12
PBL (m)
1600
1200
800
Gas- / Particle-phase Primary emitted
10
8
6
HOA mass conc. (µg m-3)
14
12
10
8
6
4
2
0
ΔHOA (µg m-3 emitted per 10 min)
0.6
0.5
0.4
0.3
0.2
0.1
0.0
Measured HOA
Interpolated HOA
ΔHOA
Max at 1.69 µg m-3
12:00 AM
4/9/2003
3:00 AM
6:00 AM
9:00 AM
12:00 PM

Figure SI-4

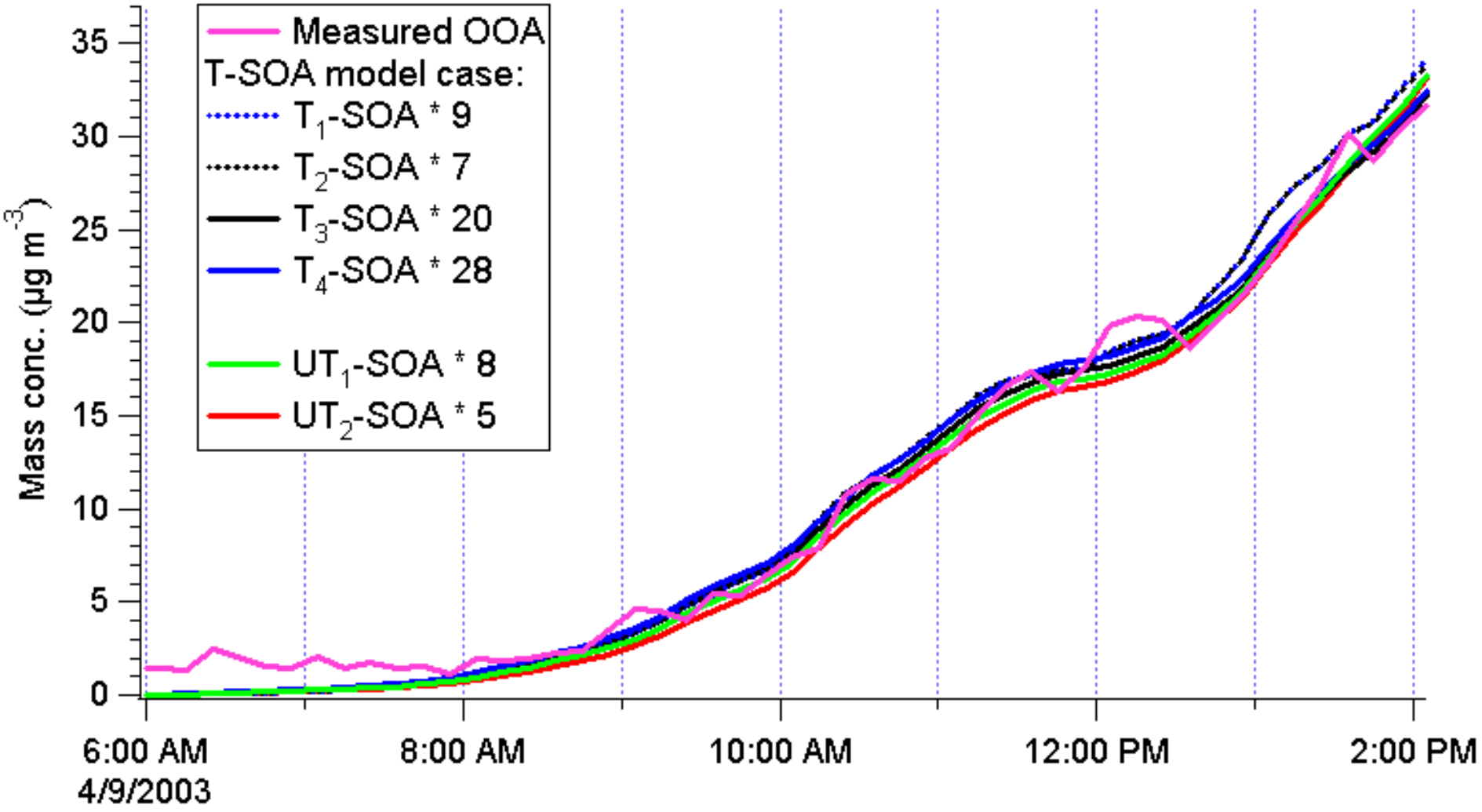
Measured OOA
T-SOA model case:
T1-SOA * 9
T2-SOA * 7
T3-SOA * 20
T4-SOA * 28
UT1-SOA * 8
UT2-SOA * 5
Mass conc. (µg m-3)
0
5
10
15
20
25
30
35
6:00 AM
4/9/2003
8:00 AM
10:00 AM
12:00 PM
2:00 PM

Figure SI-5

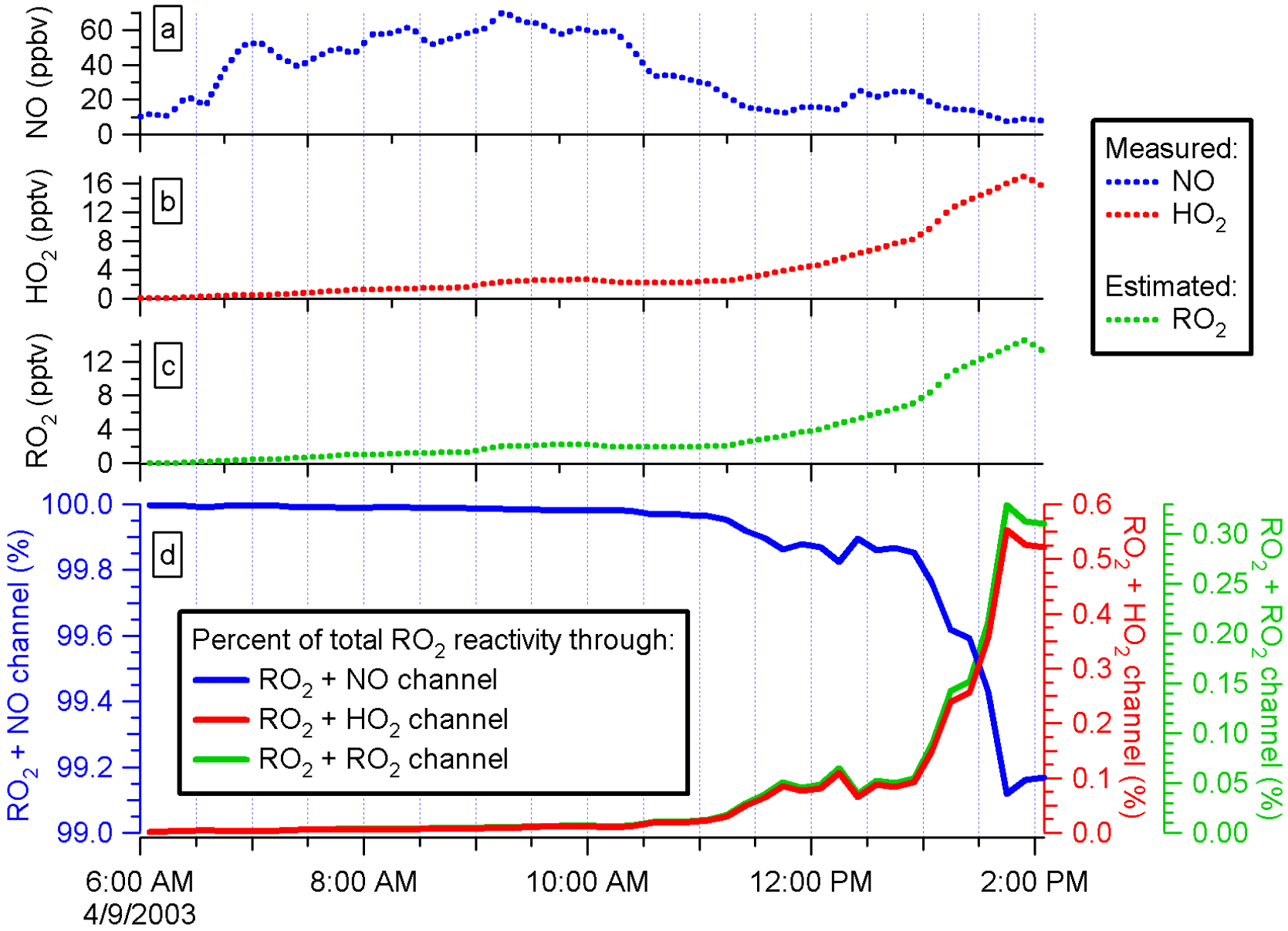
a
NO (ppbv)
60
40
20
0
b
HO2 (pptv)
16
12
8
4
0
c
RO2 (pptv)
12
8
4
0
Measured:
NO
HO2
Estimated:
RO2
d
RO2 + NO channel (%)
100.0
99.8
99.6
99.4
99.2
99.0
RO2 + HO2 channel (%)
0.6
0.5
0.4
0.3
0.2
0.1
0.0
RO2 + RO2 channel (%)
0.30
0.25
0.20
0.15
0.10
0.05
0.00
Percent of total RO2 reactivity through:
RO2 + NO channel
RO2 + HO2 channel
RO2 + RO2 channel
6:00 AM
4/9/2003
8:00 AM
10:00 AM
12:00 PM
2:00 PM

Figure SI-6

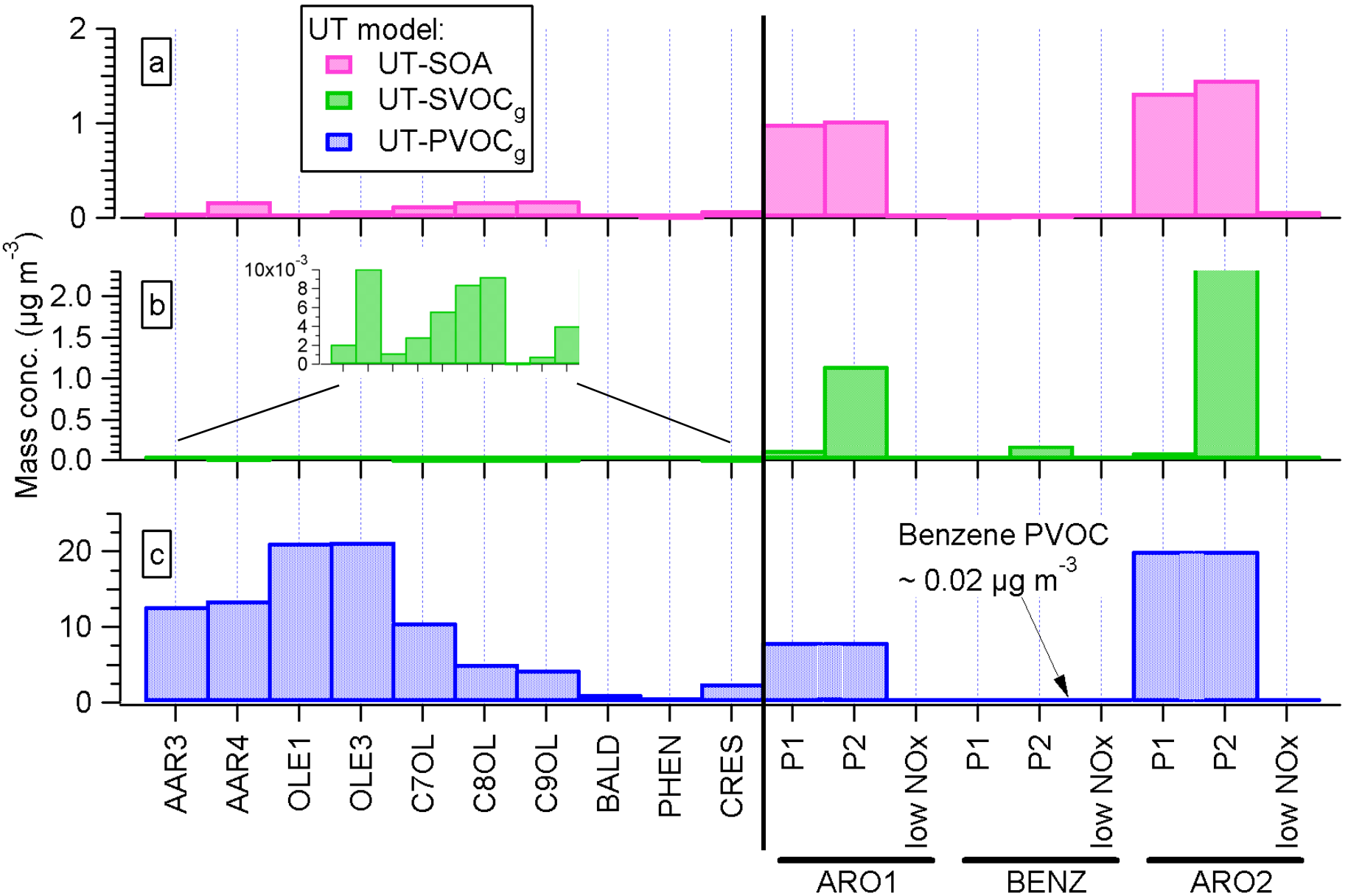
UT model:
UT-SOA
UT-SVOC$_g$
UT-PVOC$_g$
a
b
c
10x10^{-3}
Mass conc. (µg m^{-3})
Benzene PVOC
~ 0.02 µg m^{-3}
AAR3
AAR4
OLE1
OLE3
C7OL
C8OL
C9OL
BALD
PHEN
CRES
P1
P2
low NOx
ARO1
BENZ
ARO2

Figure SI-7

Day of MCMA-2003	Meas. OOA / Model SOA @ 10 am	
	T3-SOA case	UT1-SOA case
4/9/2003	8.5	8.3
4/10/2003	9	6.6
4/13/2003	5.2	4
4/14/2003	8.1	5.7
4/22/2003	9.7	7

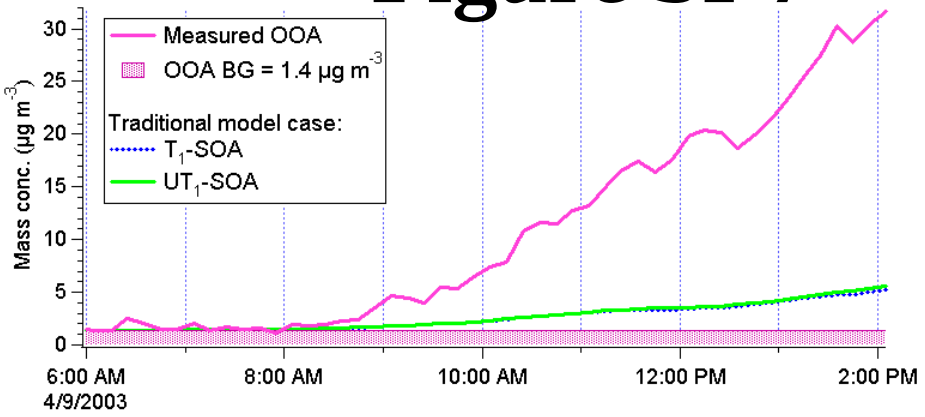

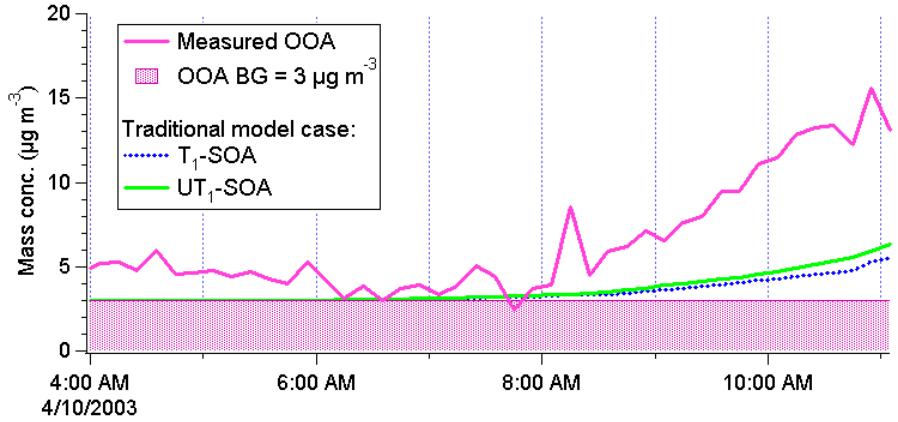

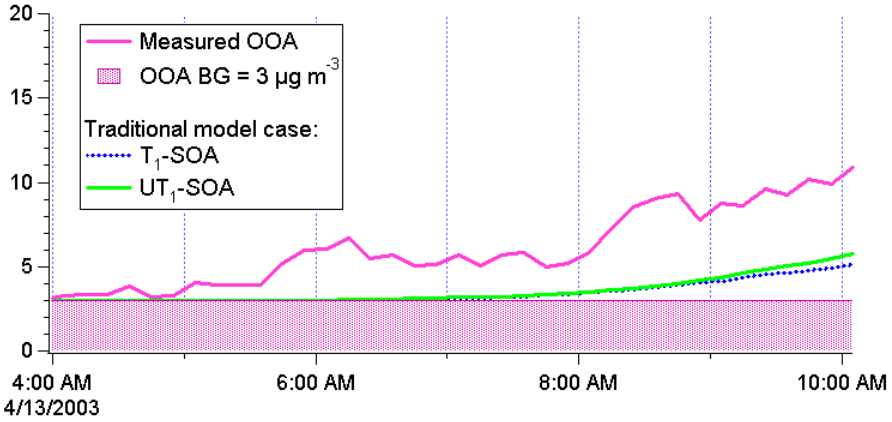

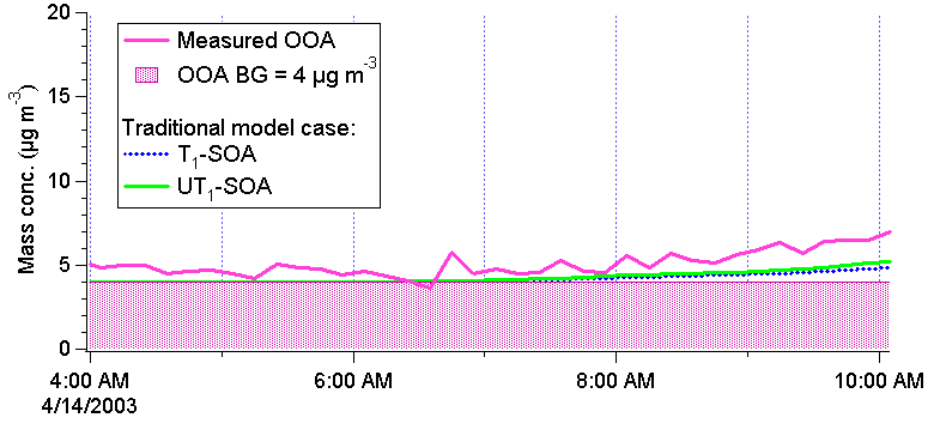

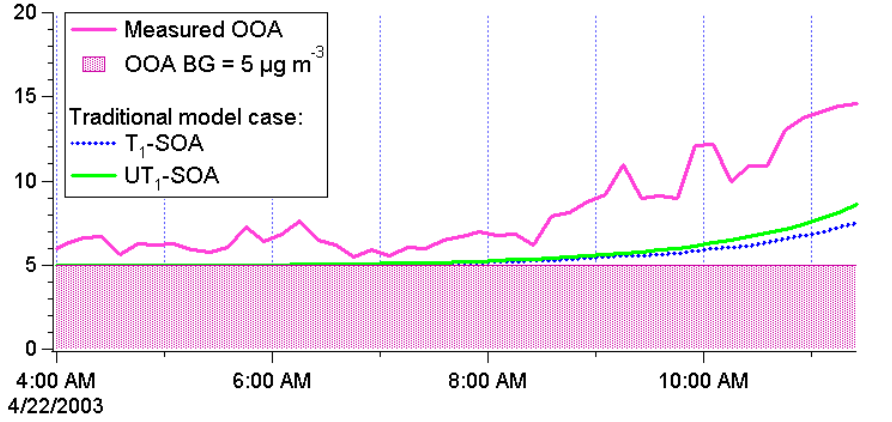

Figure SI-8

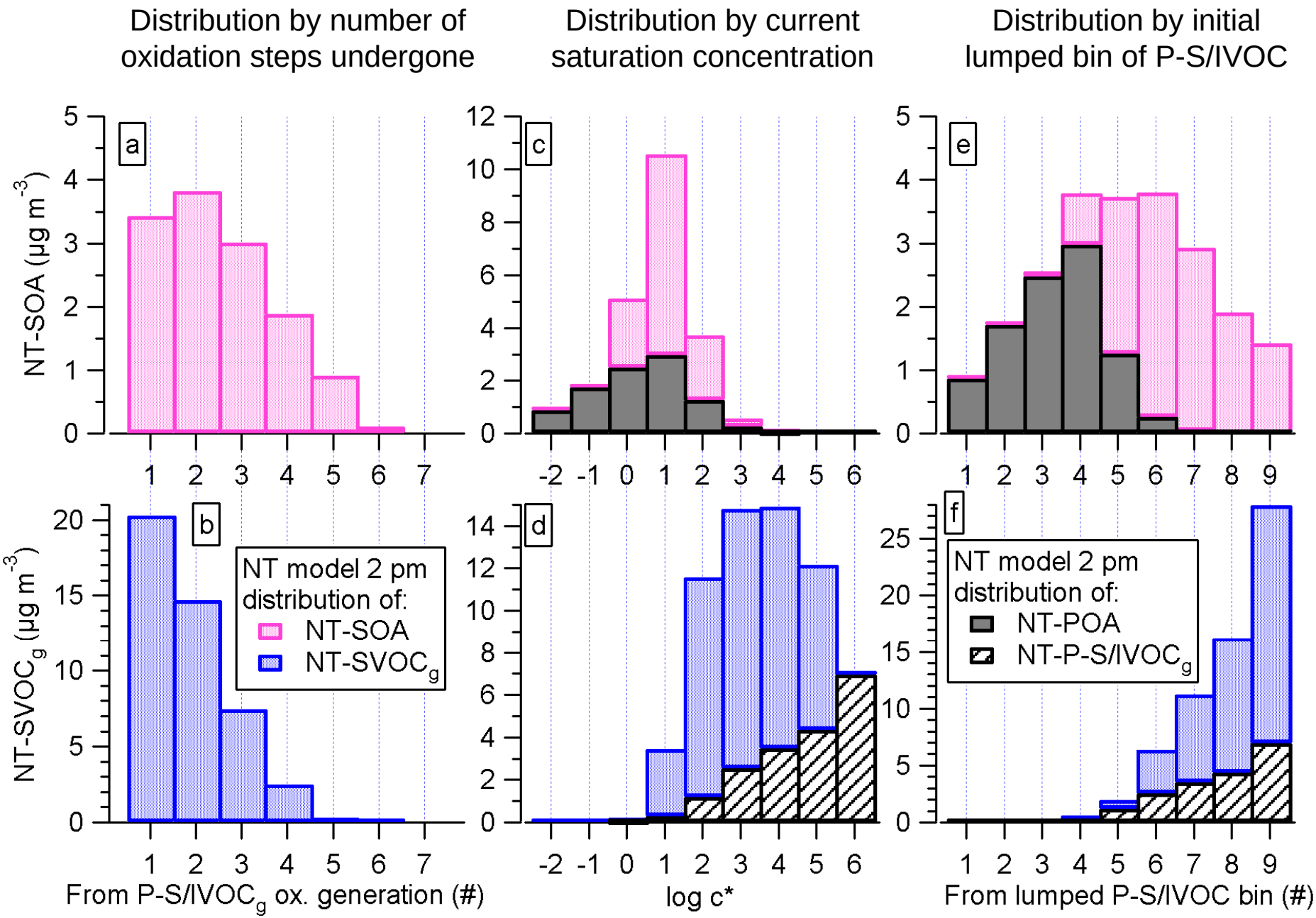
Distribution by number of oxidation steps undergone
Distribution by current saturation concentration
Distribution by initial lumped bin of P-S/IVOC
a
b
c
d
e
f
NT-SOA (µg m-3)
NT-SVOCg (µg m-3)
NT model 2 pm distribution of:
NT-SOA
NT-SVOCg
NT model 2 pm distribution of:
NT-POA
NT-P-S/IVOCg
From P-S/IVOCg ox. generation (#)
log c*
From lumped P-S/IVOC bin (#)

Figure SI-9

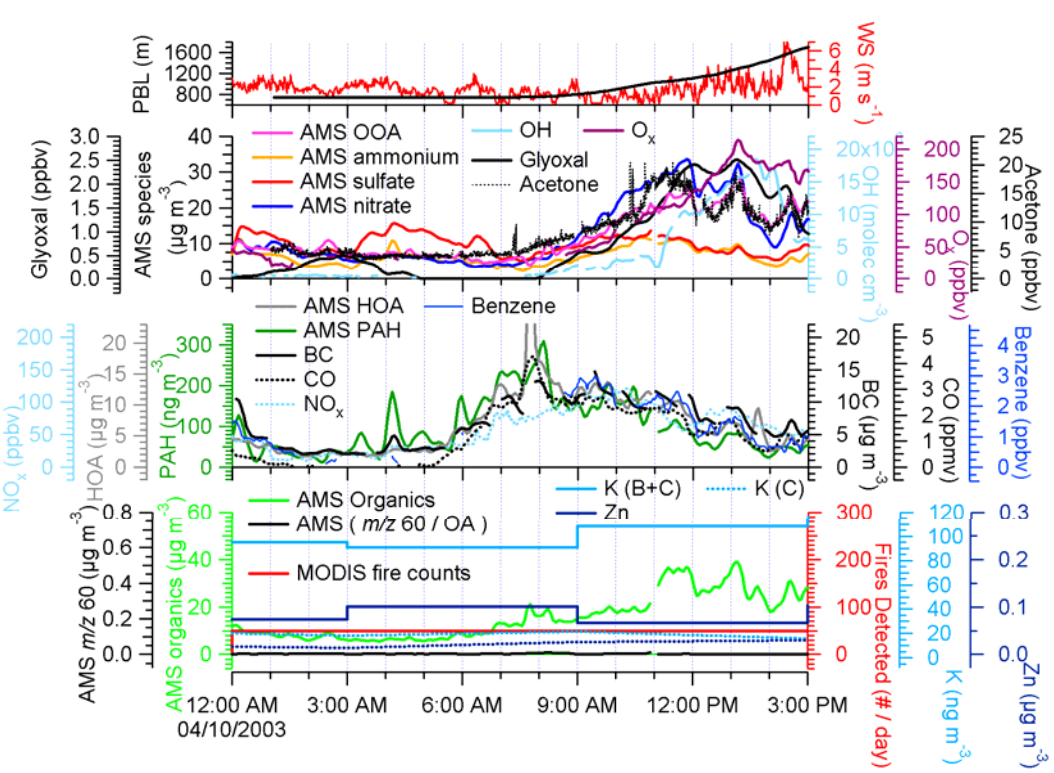
PBL (m)
WS (m s-1)
Glyoxal (ppbv)
AMS species (μg m-3)
AMS OOA
AMS ammonium
AMS sulfate
AMS nitrate
OH
Ox
Glyoxal
Acetone
OH (molec cm-3)
Ox (ppbv)
Acetone (ppbv)
NOx (ppbv)
HOA (μg m-3)
AMS HOA
AMS PAH
BC
CO
NOx
Benzene
PAH (ng m-3)
BC (μg m-3)
CO (ppmv)
Benzene (ppbv)
AMS m/z 60 (μg m-3)
AMS organics (μg m-3)
AMS Organics
AMS (m/z 60 / OA)
MODIS fire counts
K (B+C)
K (C)
Zn
Fires Detected (# / day)
K (ng m-3)
Zn (μg m-3)
12:00 AM
04/10/2003
3:00 AM
6:00 AM
9:00 AM
12:00 PM
3:00 PM

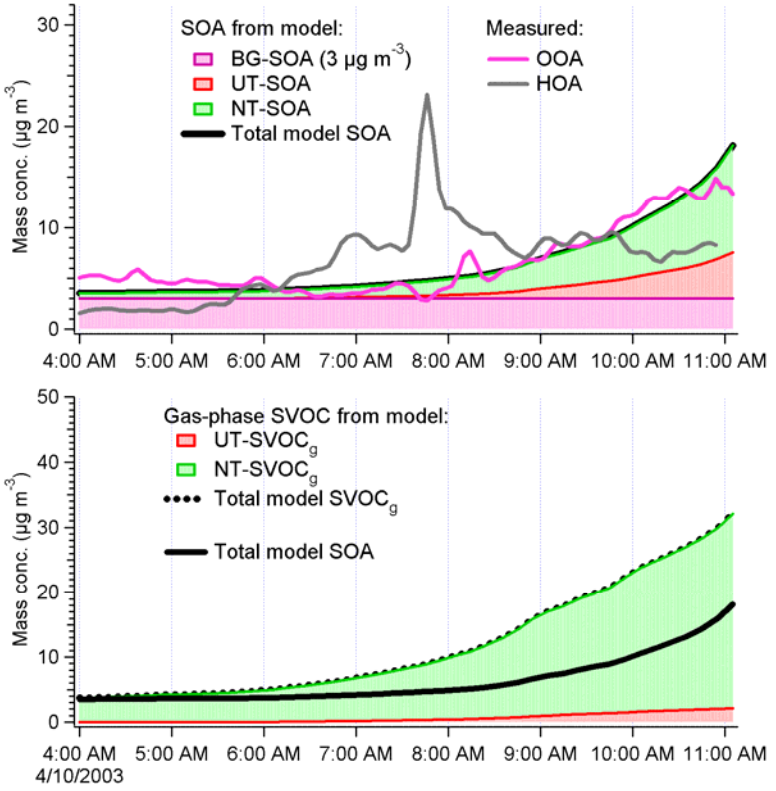
SOA from model:
BG-SOA (3 μg m-3)
UT-SOA
NT-SOA
Total model SOA
Measured:
OOA
HOA
Mass conc. (μg m-3)
4:00 AM
5:00 AM
6:00 AM
7:00 AM
8:00 AM
9:00 AM
10:00 AM
11:00 AM
Gas-phase SVOC from model:
UT-SVOCg
NT-SVOCg
Total model SVOCg
Total model SOA
4/10/2003

Figure SI-10

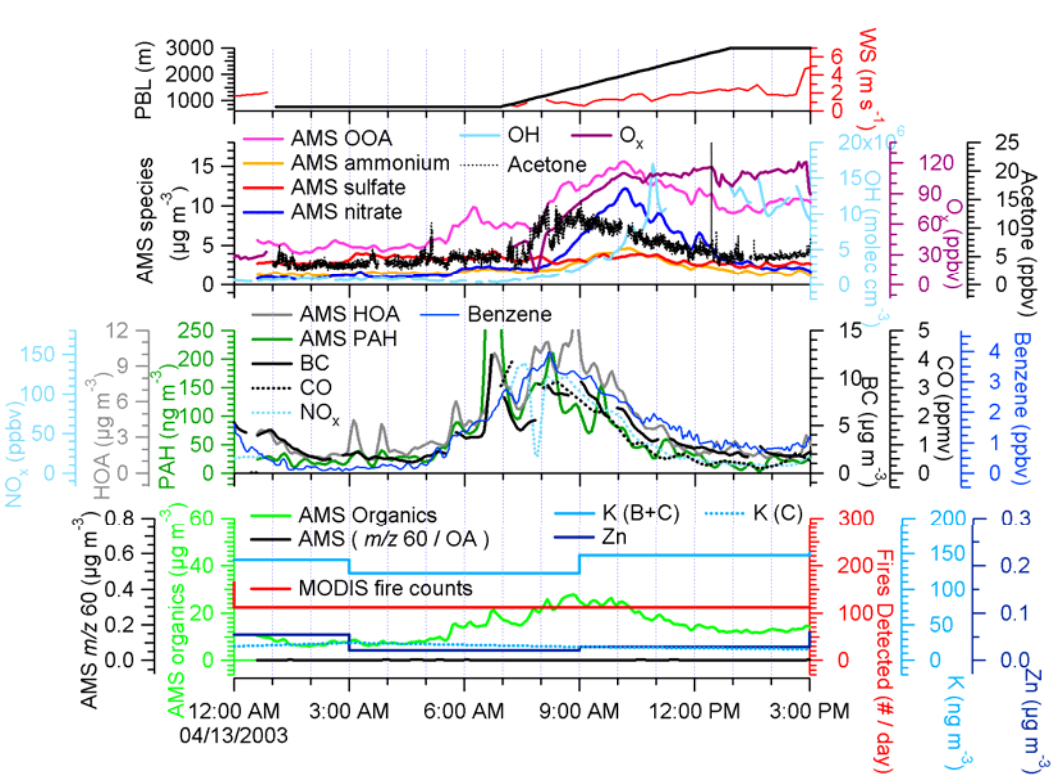
PBL (m)
WS (m s-1)
AMS species (µg m-3)
AMS OOA
AMS ammonium
AMS sulfate
AMS nitrate
OH
Ox
Acetone
OH (molec cm-3)
Ox (ppbv)
Acetone (ppbv)
AMS HOA
AMS PAH
BC
CO
NOx
Benzene
NOx (ppbv)
HOA (µg m-3)
PAH (ng m-3)
BC (µg m-3)
CO (ppmv)
Benzene (ppbv)
AMS Organics
AMS (m/z 60 / OA)
K (B+C)
K (C)
Zn
MODIS fire counts
AMS m/z 60 (µg m-3)
AMS organics (µg m-3)
Fires Detected (# / day)
K (ng m-3)
Zn (µg m-3)
12:00 AM
04/13/2003
3:00 AM
6:00 AM
9:00 AM
12:00 PM
3:00 PM

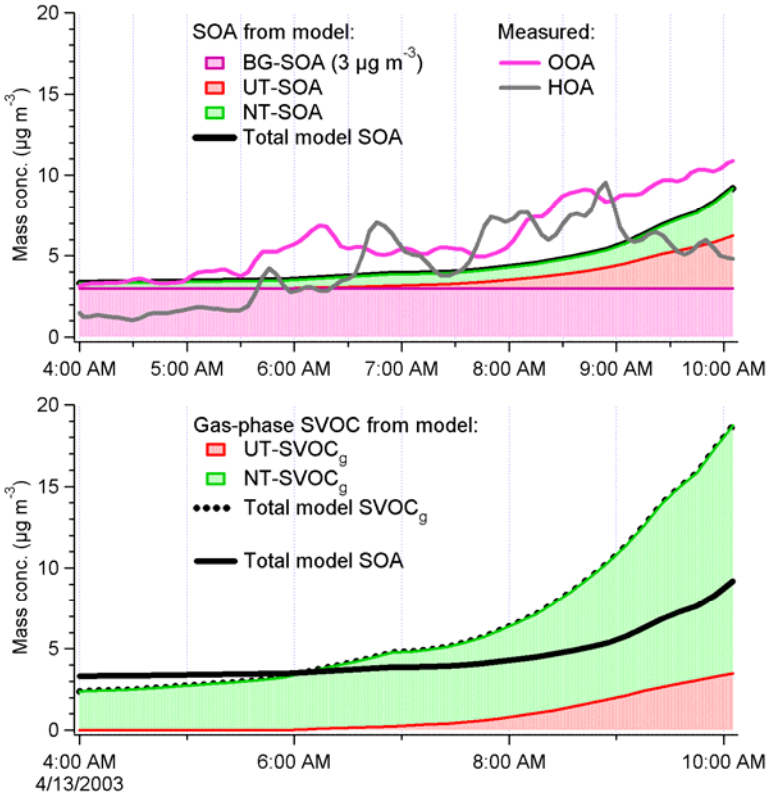
SOA from model:
BG-SOA (3 µg m-3)
UT-SOA
NT-SOA
Total model SOA
Measured:
OOA
HOA
Mass conc. (µg m-3)
4:00 AM
5:00 AM
6:00 AM
7:00 AM
8:00 AM
9:00 AM
10:00 AM
Gas-phase SVOC from model:
UT-SVOCg
NT-SVOCg
Total model SVOCg
Total model SOA
4:00 AM
4/13/2003

Figure SI-11

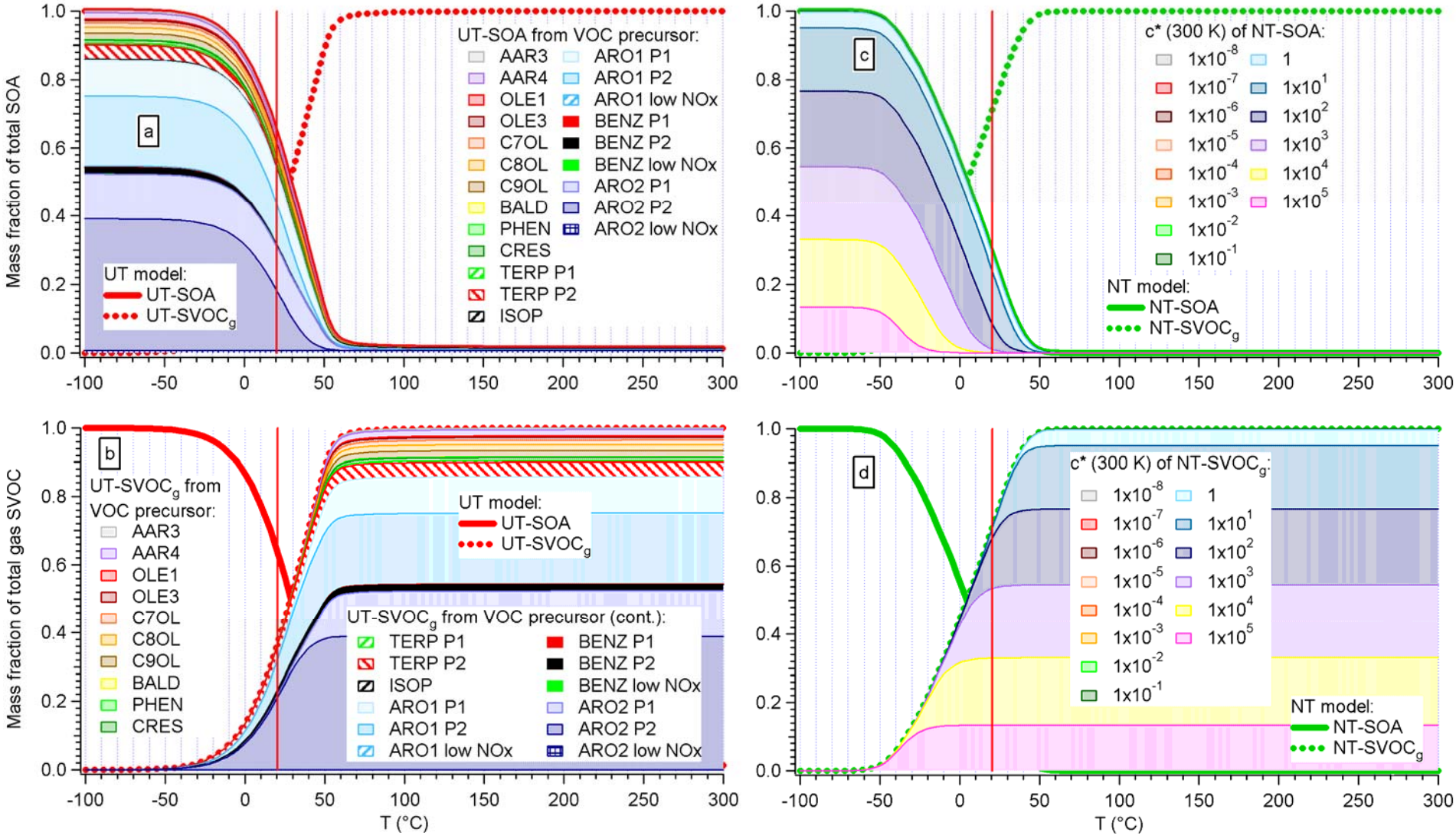
a
Mass fraction of total SOA
UT-SOA from VOC precursor:
AAR3
AAR4
OLE1
OLE3
C7OL
C8OL
C9OL
BALD
PHEN
CRES
TERP P1
TERP P2
ISOP
ARO1 P1
ARO1 P2
ARO1 low NOx
BENZ P1
BENZ P2
BENZ low NOx
ARO2 P1
ARO2 P2
ARO2 low NOx
UT model:
UT-SOA
UT-SVOCg
c
c* (300 K) of NT-SOA:
1x10-8
1x10-7
1x10-6
1x10-5
1x10-4
1x10-3
1x10-2
1x10-1
1
1x101
1x102
1x103
1x104
1x105
NT model:
NT-SOA
NT-SVOCg
b
Mass fraction of total gas SVOC
UT-SVOCg from VOC precursor:
UT-SVOCg from VOC precursor (cont.):
T (°C)
d
c* (300 K) of NT-SVOCg:

Figure SI-12

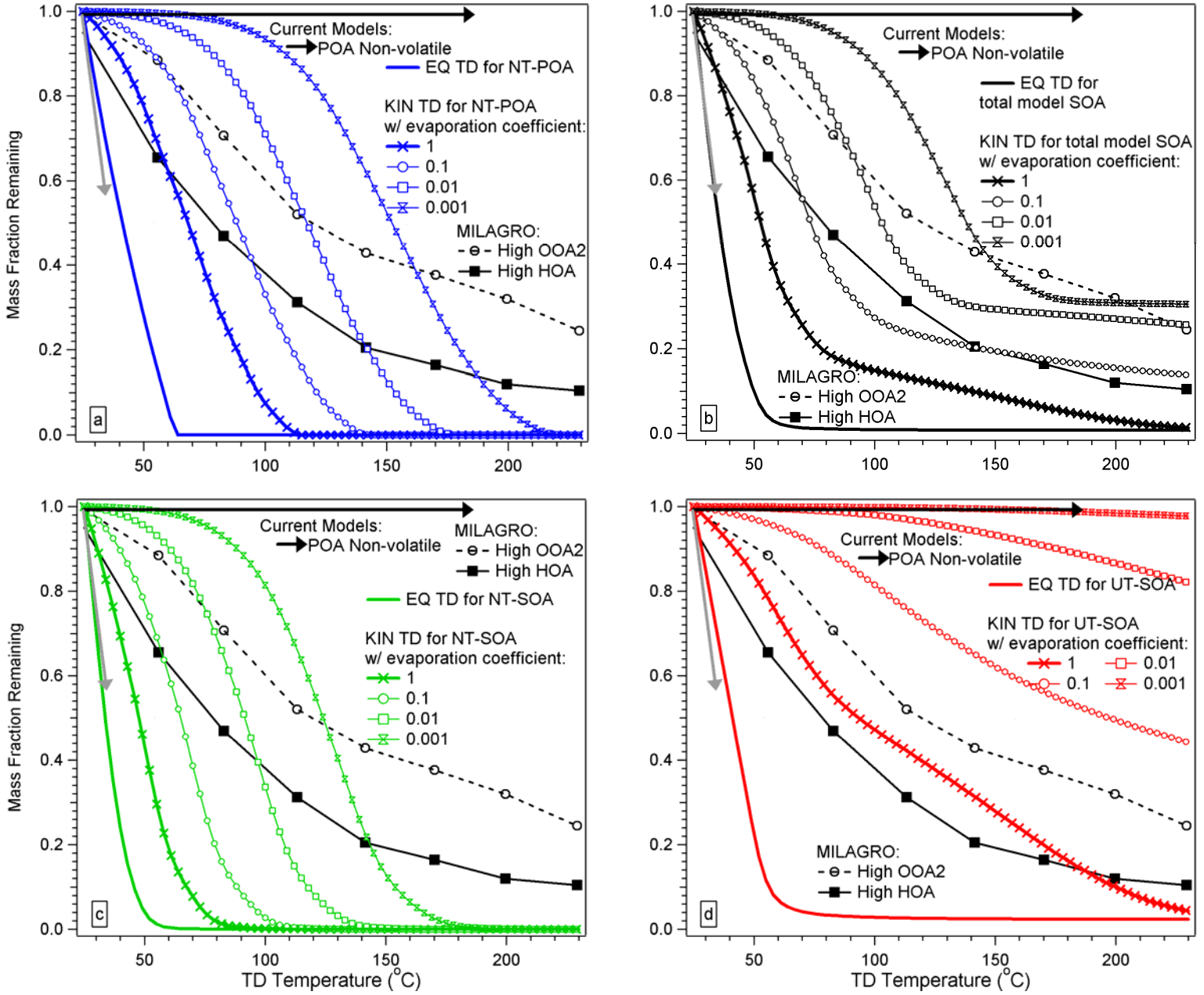
Mass Fraction Remaining
TD Temperature (°C)
Current Models:
POA Non-volatile
EQ TD for NT-POA
KIN TD for NT-POA
w/ evaporation coefficient:
1
0.1
0.01
0.001
MILAGRO:
High OOA2
High HOA
a
EQ TD for
total model SOA
KIN TD for total model SOA
b
EQ TD for NT-SOA
KIN TD for NT-SOA
c
EQ TD for UT-SOA
KIN TD for UT-SOA
d

Figure SI-13

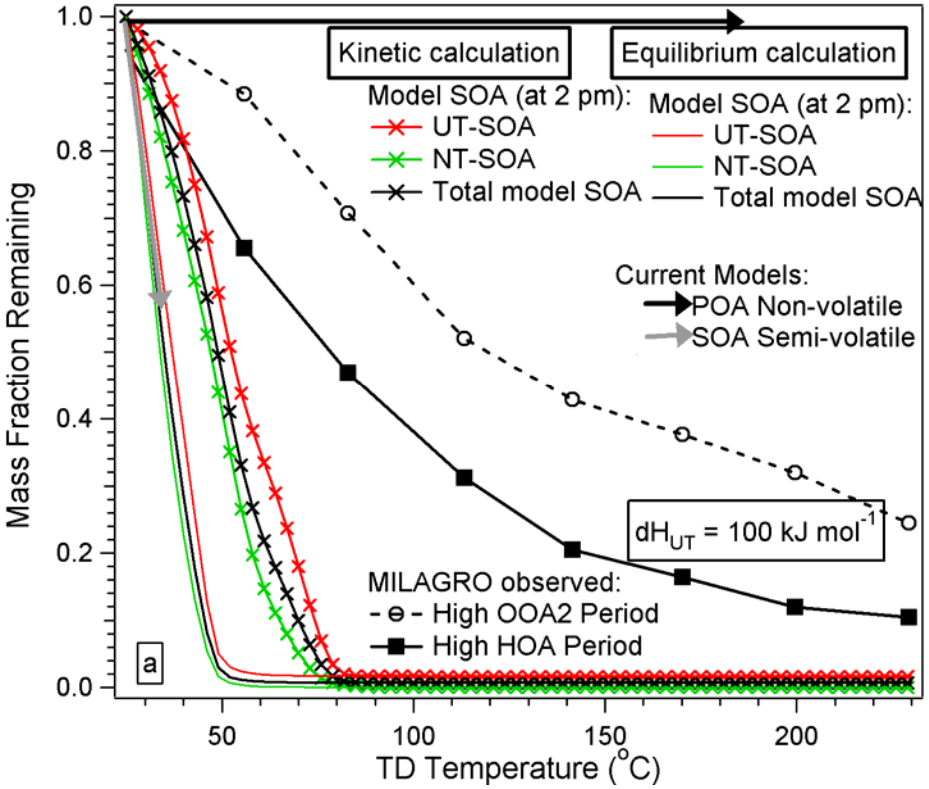
Kinetic calculation
Equilibrium calculation
Model SOA (at 2 pm):
UT-SOA
NT-SOA
Total model SOA
Model SOA (at 2 pm):
UT-SOA
NT-SOA
Total model SOA
Current Models:
POA Non-volatile
SOA Semi-volatile
dH$_{UT}$ = 100 kJ mol^{-1}
MILAGRO observed:
High OOA2 Period
High HOA Period
a
Mass Fraction Remaining
TD Temperature (°C)
1.0
0.8
0.6
0.4
0.2
0.0
50
100
150
200

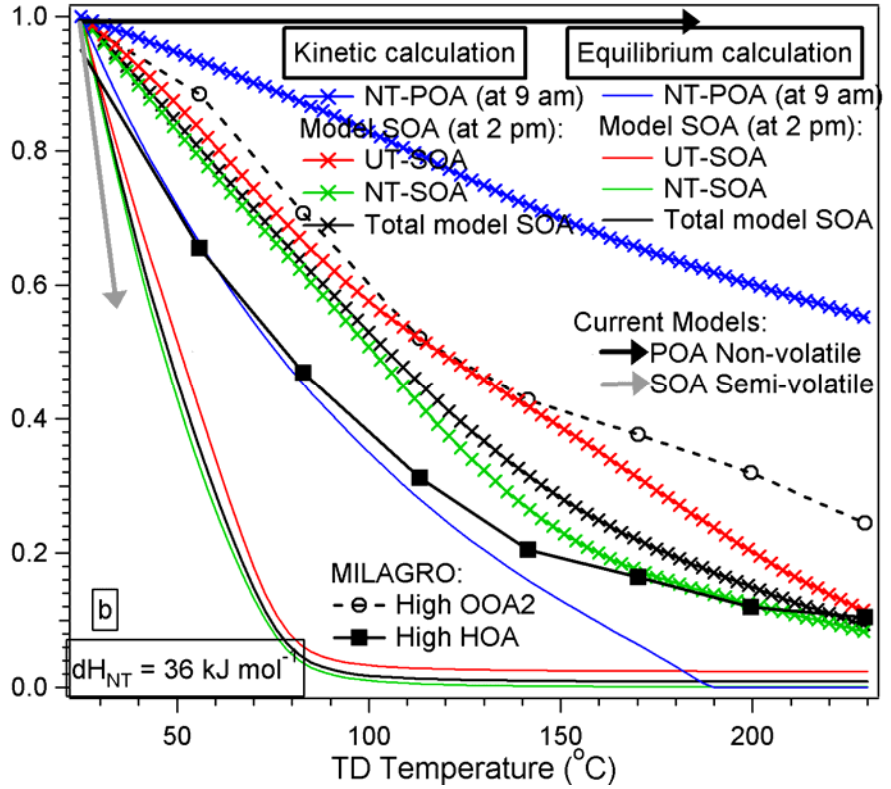
Kinetic calculation
Equilibrium calculation
NT-POA (at 9 am)
NT-POA (at 9 am)
Model SOA (at 2 pm):
UT-SOA
NT-SOA
Total model SOA
Model SOA (at 2 pm):
UT-SOA
NT-SOA
Total model SOA
Current Models:
POA Non-volatile
SOA Semi-volatile
MILAGRO:
High OOA2
High HOA
b
dH$_{NT}$ = 36 kJ mol^{-1}
TD Temperature (°C)
1.0
0.8
0.6
0.4
0.2
0.0
50
100
150
200

Figure SI-14

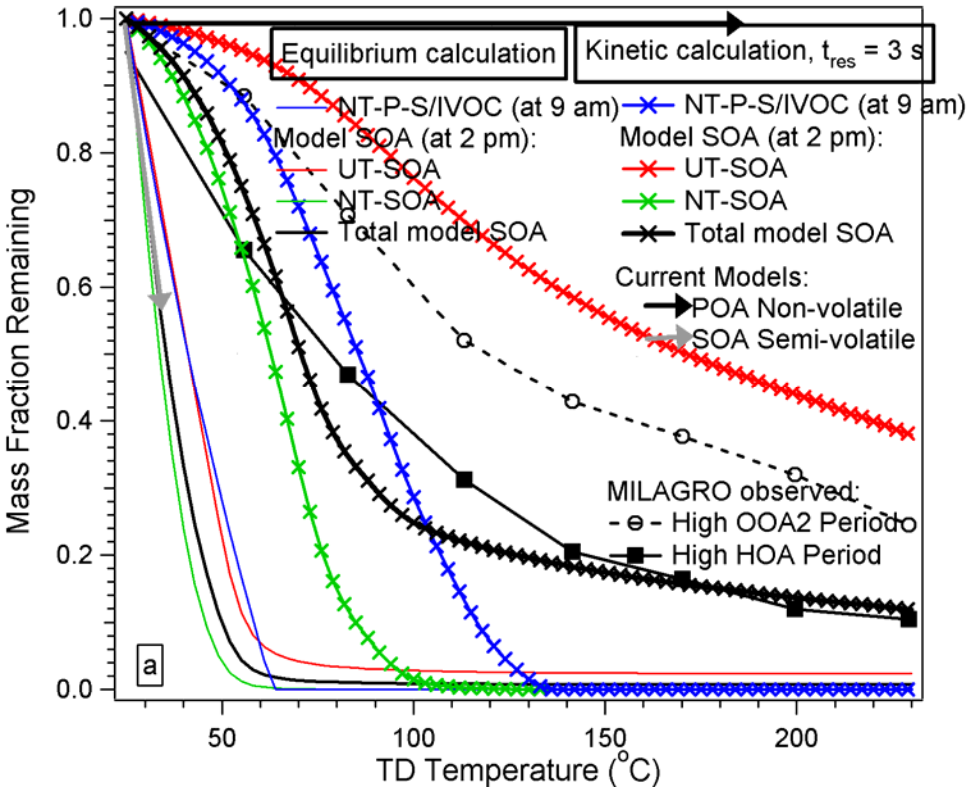
Equilibrium calculation
Kinetic calculation, t_{res} = 3 s
NT-P-S/IVOC (at 9 am)
NT-P-S/IVOC (at 9 am)
Model SOA (at 2 pm):
UT-SOA
NT-SOA
Total model SOA
Model SOA (at 2 pm):
UT-SOA
NT-SOA
Total model SOA
Current Models:
POA Non-volatile
SOA Semi-volatile
MILAGRO observed:
High OOA2 Period
High HOA Period
a
Mass Fraction Remaining
TD Temperature (°C)
1.0
0.8
0.6
0.4
0.2
0.0
50
100
150
200

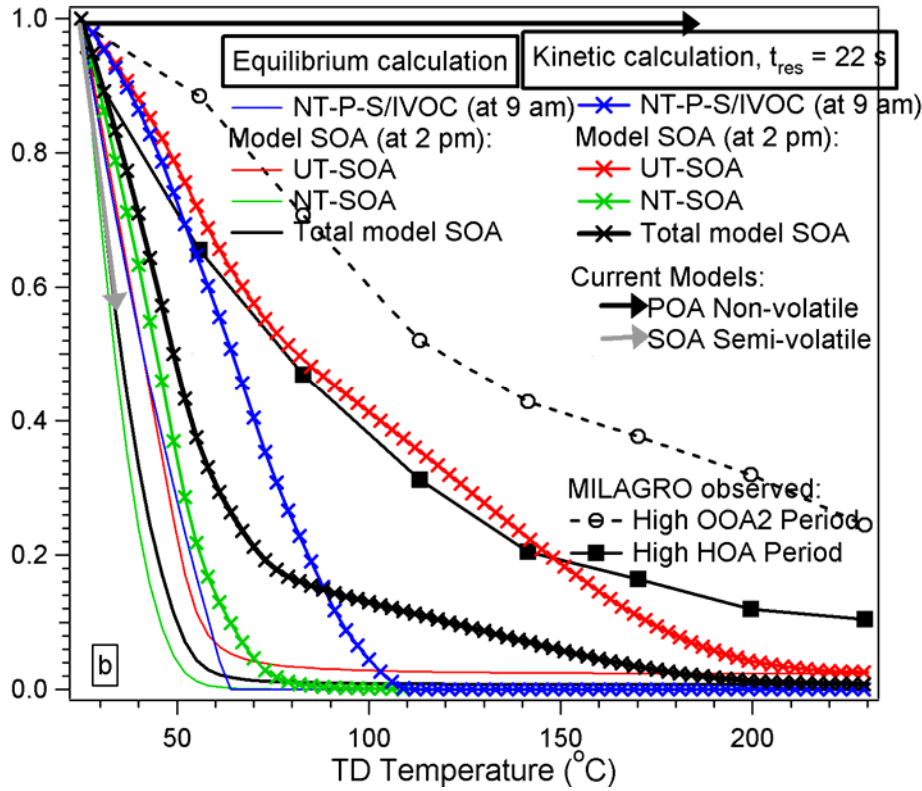
Equilibrium calculation
Kinetic calculation, t_{res} = 22 s
NT-P-S/IVOC (at 9 am)
NT-P-S/IVOC (at 9 am)
Model SOA (at 2 pm):
UT-SOA
NT-SOA
Total model SOA
Model SOA (at 2 pm):
UT-SOA
NT-SOA
Total model SOA
Current Models:
POA Non-volatile
SOA Semi-volatile
MILAGRO observed:
High OOA2 Period
High HOA Period
b
TD Temperature (°C)
1.0
0.8
0.6
0.4
0.2
0.0
50
100
150
200

Figure SI-15

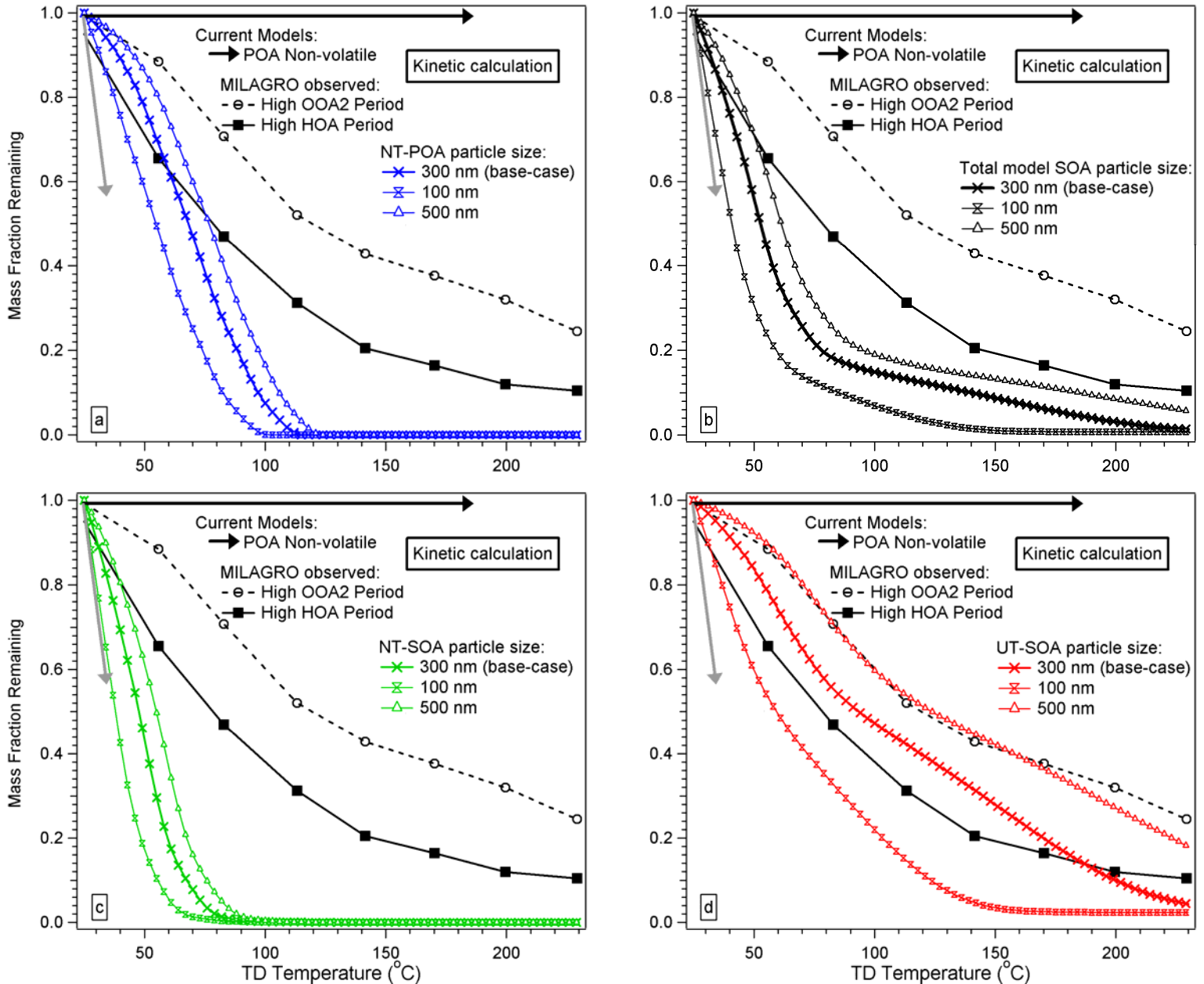
Mass Fraction Remaining
TD Temperature (°C)
Current Models:
POA Non-volatile
Kinetic calculation
MILAGRO observed:
High OOA2 Period
High HOA Period
NT-POA particle size:
300 nm (base-case)
100 nm
500 nm
Total model SOA particle size:
NT-SOA particle size:
UT-SOA particle size:
a
b
c
d

Figure SI-16

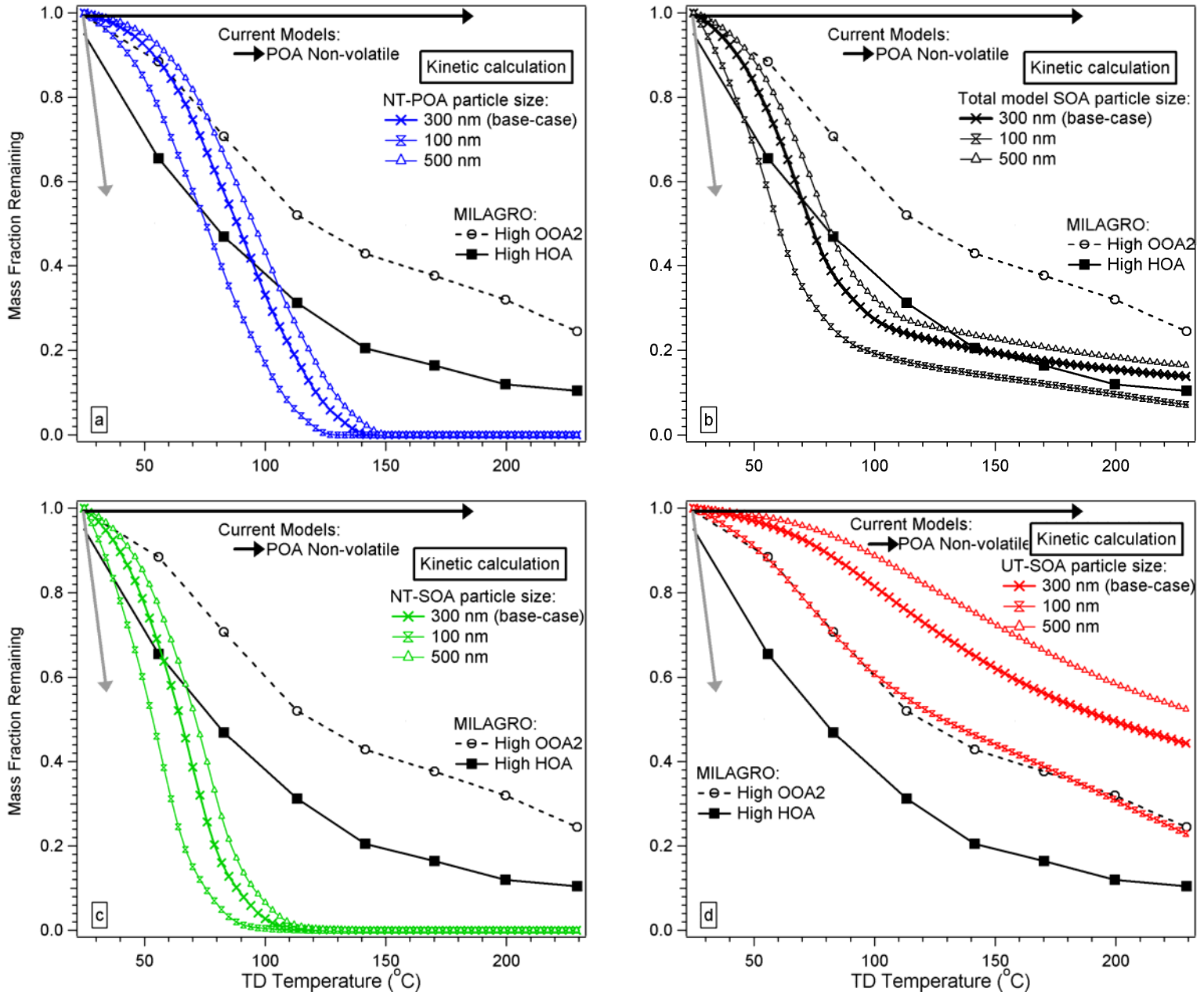
Mass Fraction Remaining
TD Temperature (°C)
Current Models:
POA Non-volatile
Kinetic calculation
NT-POA particle size:
300 nm (base-case)
100 nm
500 nm
MILAGRO:
High OOA2
High HOA
a
Total model SOA particle size:
b
NT-SOA particle size:
c
UT-SOA particle size:
d

Figure SI-17

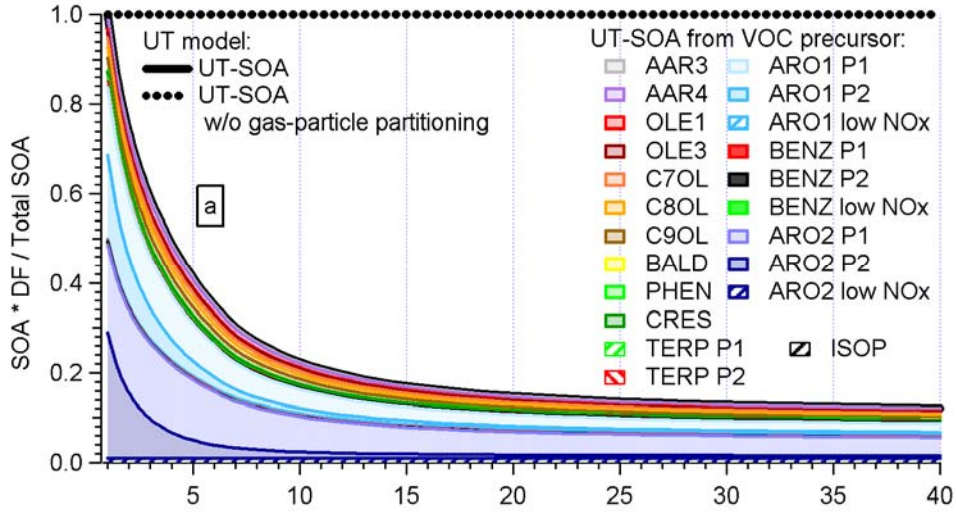
a
UT model:
UT-SOA
UT-SOA
w/o gas-particle partitioning
UT-SOA from VOC precursor:
AAR3
AAR4
OLE1
OLE3
C7OL
C8OL
C9OL
BALD
PHEN
CRES
TERP P1
TERP P2
ARO1 P1
ARO1 P2
ARO1 low NOx
BENZ P1
BENZ P2
BENZ low NOx
ARO2 P1
ARO2 P2
ARO2 low NOx
ISOP
SOA * DF / Total SOA

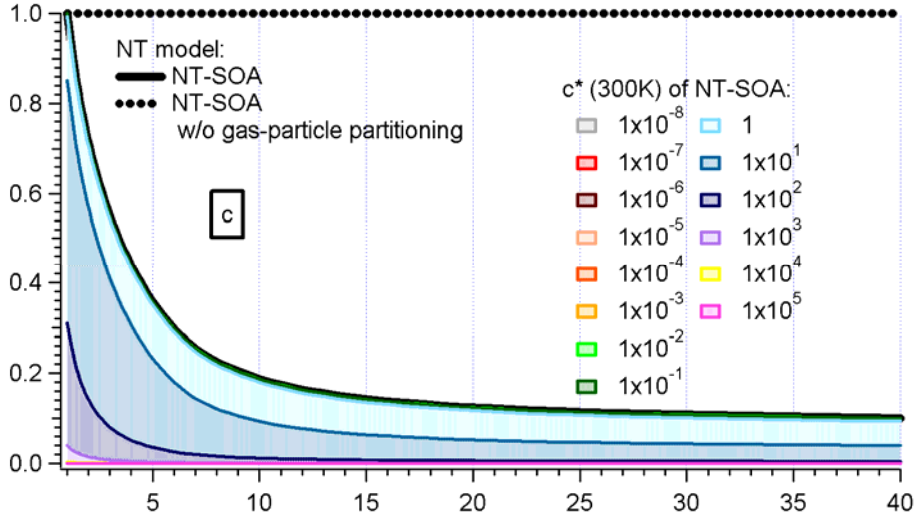
c
NT model:
NT-SOA
NT-SOA
w/o gas-particle partitioning
c* (300K) of NT-SOA:
1x10-8
1x10-7
1x10-6
1x10-5
1x10-4
1x10-3
1x10-2
1x10-1
1
1x101
1x102
1x103
1x104
1x105

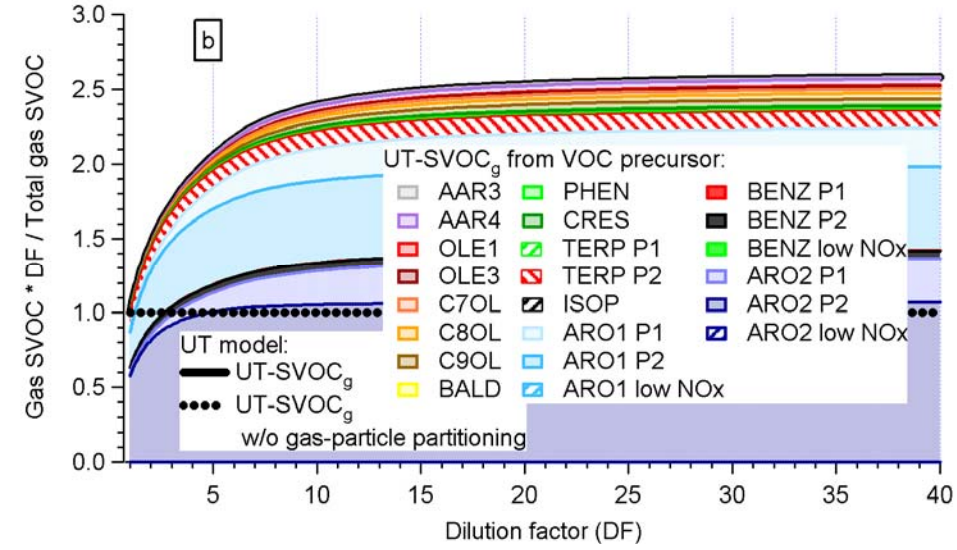
b
UT-SVOCg from VOC precursor:
AAR3
AAR4
OLE1
OLE3
C7OL
C8OL
C9OL
BALD
PHEN
CRES
TERP P1
TERP P2
ISOP
ARO1 P1
ARO1 P2
ARO1 low NOx
BENZ P1
BENZ P2
BENZ low NOx
ARO2 P1
ARO2 P2
ARO2 low NOx
UT model:
UT-SVOCg
UT-SVOCg
w/o gas-particle partitioning
Gas SVOC * DF / Total gas SVOC
Dilution factor (DF)

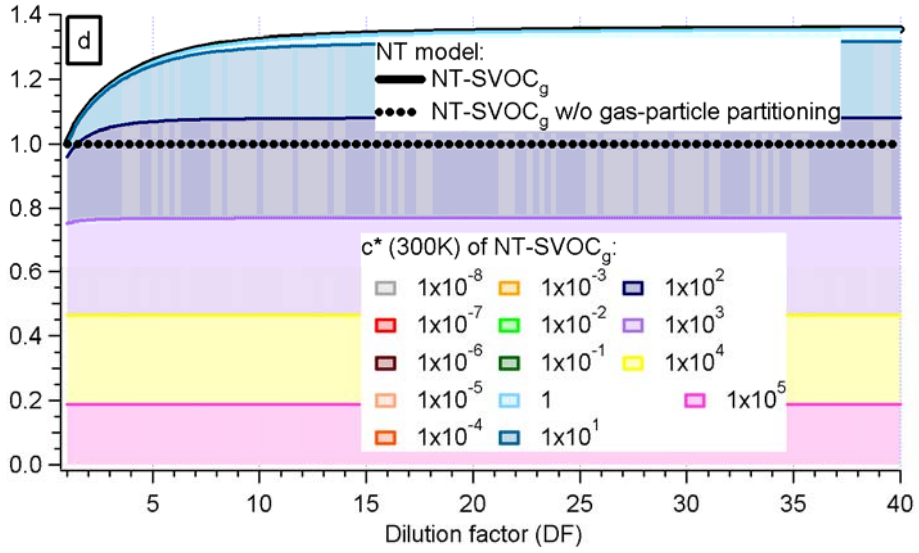
d
NT model:
NT-SVOCg
NT-SVOCg w/o gas-particle partitioning
c* (300K) of NT-SVOCg:
1x10-8
1x10-7
1x10-6
1x10-5
1x10-4
1x10-3
1x10-2
1x10-1
1
1x101
1x102
1x103
1x104
1x105
Dilution factor (DF)

Figure SI-18

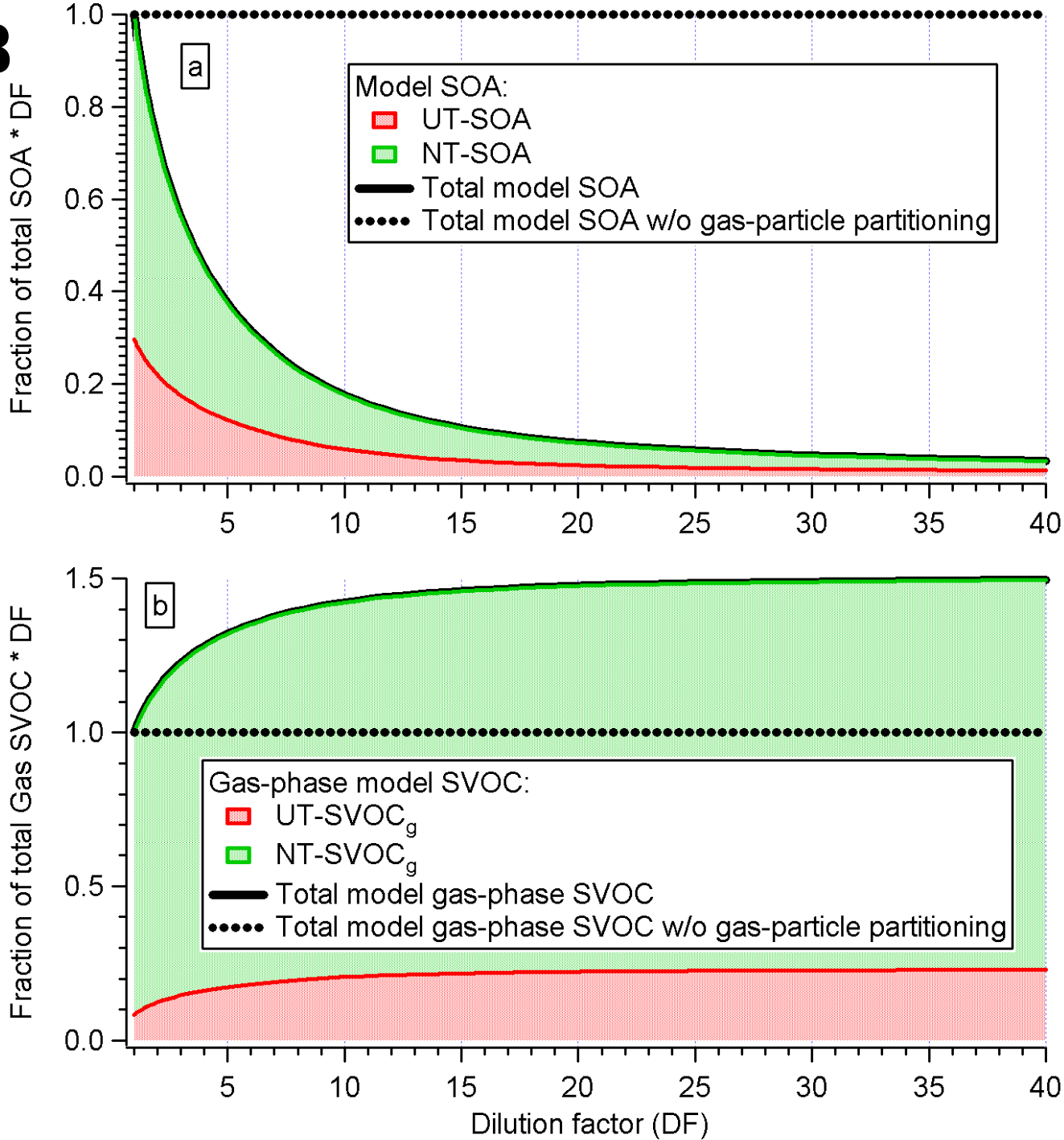
a
Model SOA:
UT-SOA
NT-SOA
Total model SOA
Total model SOA w/o gas-particle partitioning
Fraction of total SOA * DF
1.0
0.8
0.6
0.4
0.2
0.0
5
10
15
20
25
30
35
40
b
Gas-phase model SVOC:
UT-SVOC$_g$
NT-SVOC$_g$
Total model gas-phase SVOC
Total model gas-phase SVOC w/o gas-particle partitioning
Fraction of total Gas SVOC * DF
1.5
1.0
0.5
0.0
Dilution factor (DF)

Figure SI-19

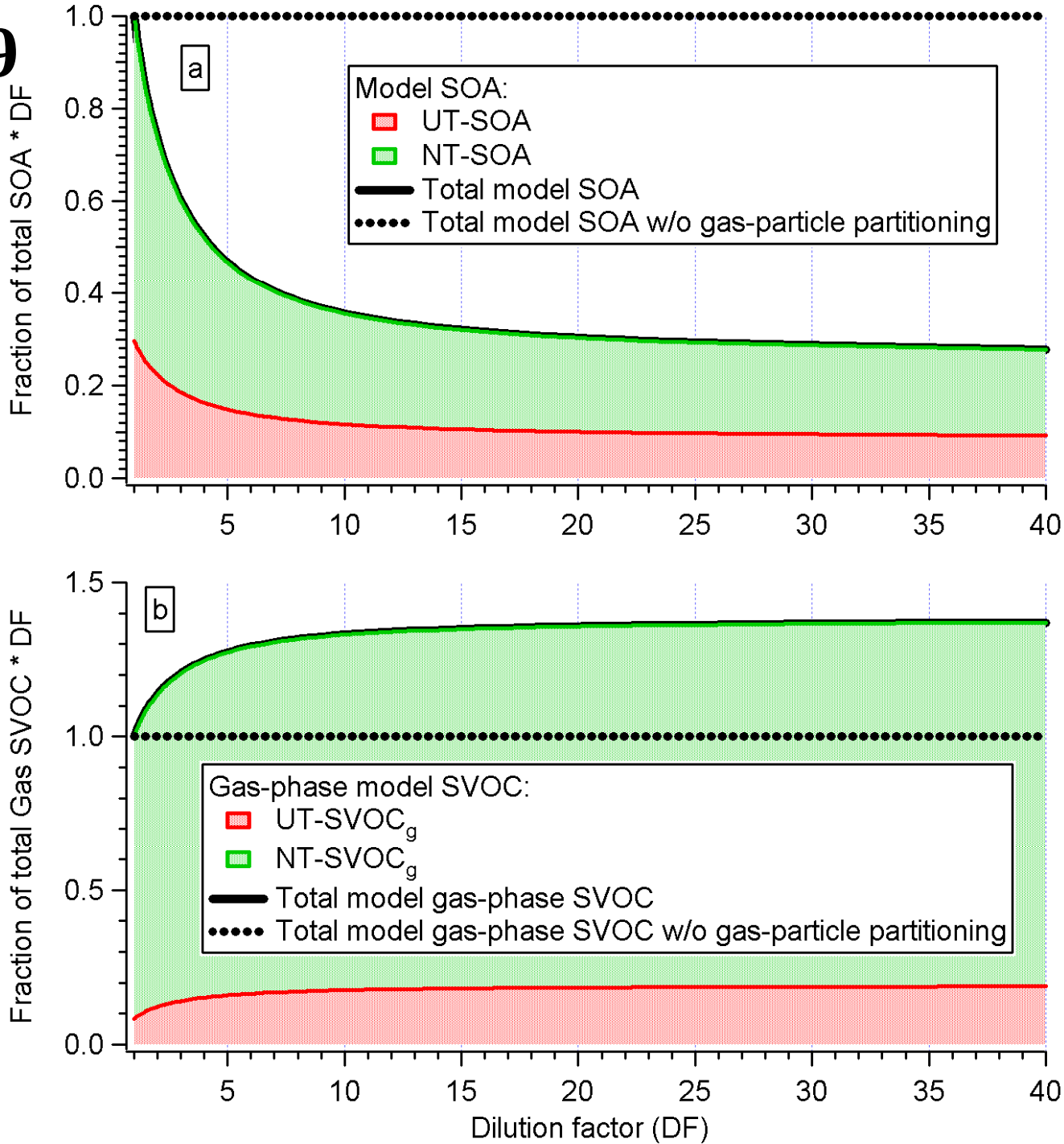
a
Model SOA:
UT-SOA
NT-SOA
Total model SOA
Total model SOA w/o gas-particle partitioning
Fraction of total SOA * DF
1.0
0.8
0.6
0.4
0.2
0.0
5
10
15
20
25
30
35
40
b
Gas-phase model SVOC:
UT-SVOC$_g$
NT-SVOC$_g$
Total model gas-phase SVOC
Total model gas-phase SVOC w/o gas-particle partitioning
Fraction of total Gas SVOC * DF
1.5
1.0
0.5
0.0
Dilution factor (DF)

Figure SI-20

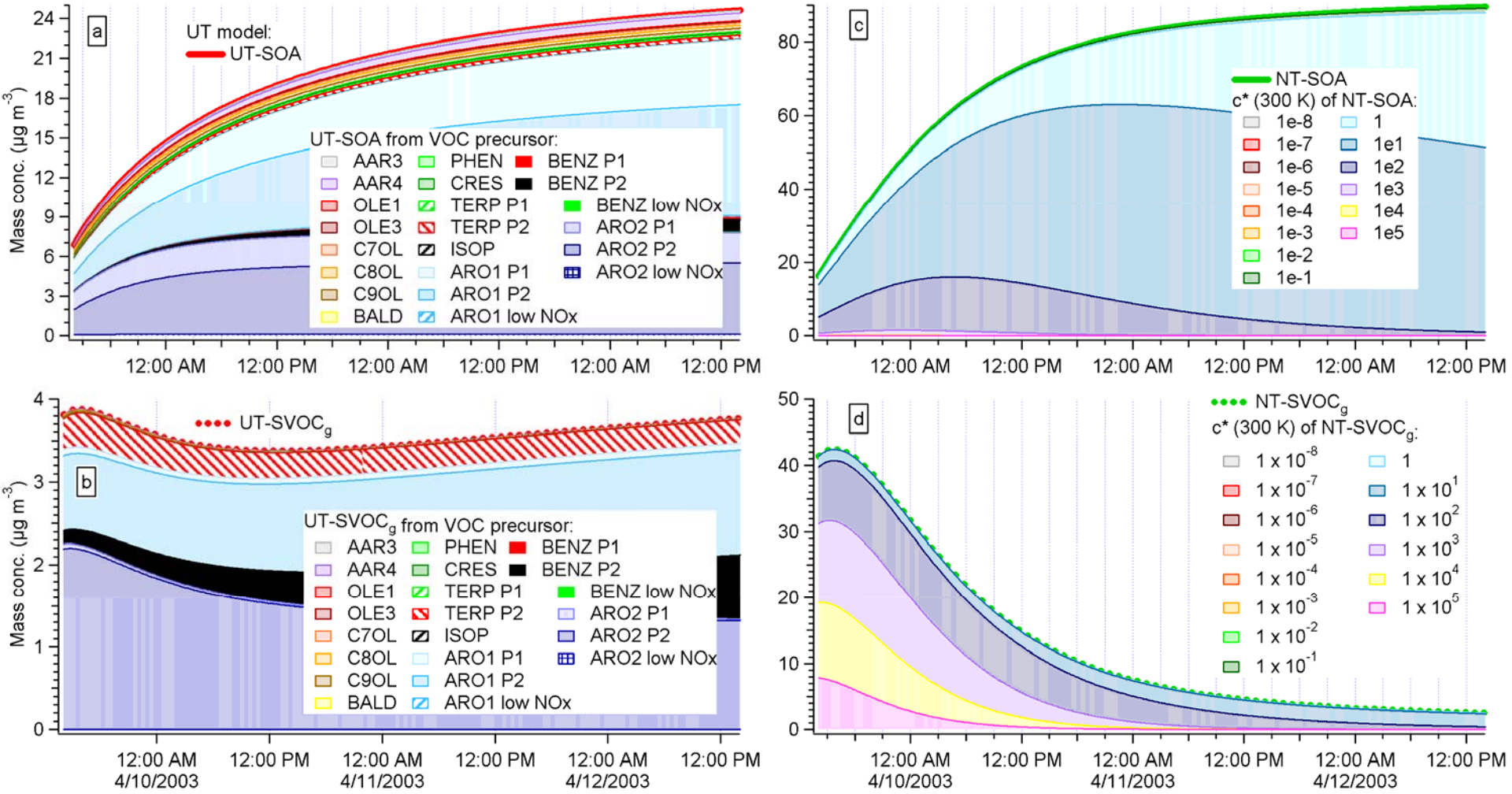
a
UT model:
UT-SOA
UT-SOA from VOC precursor:
AAR3
AAR4
OLE1
OLE3
C7OL
C8OL
C9OL
BALD
PHEN
CRES
TERP P1
TERP P2
ISOP
ARO1 P1
ARO1 P2
ARO1 low NOx
BENZ P1
BENZ P2
BENZ low NOx
ARO2 P1
ARO2 P2
ARO2 low NOx
Mass conc. (µg m-3)
0
3
6
9
12
15
18
21
24
12:00 AM
12:00 PM
12:00 AM
12:00 PM
12:00 AM
12:00 PM
c
NT-SOA
c* (300 K) of NT-SOA:
1e-8
1e-7
1e-6
1e-5
1e-4
1e-3
1e-2
1e-1
1
1e1
1e2
1e3
1e4
1e5
0
20
40
60
80
12:00 AM
12:00 PM
12:00 AM
12:00 PM
12:00 AM
12:00 PM
b
UT-SVOCg
UT-SVOCg from VOC precursor:
AAR3
AAR4
OLE1
OLE3
C7OL
C8OL
C9OL
BALD
PHEN
CRES
TERP P1
TERP P2
ISOP
ARO1 P1
ARO1 P2
ARO1 low NOx
BENZ P1
BENZ P2
BENZ low NOx
ARO2 P1
ARO2 P2
ARO2 low NOx
Mass conc. (µg m-3)
0
1
2
3
4
12:00 AM
4/10/2003
12:00 PM
12:00 AM
4/11/2003
12:00 PM
12:00 AM
4/12/2003
12:00 PM
d
NT-SVOCg
c* (300 K) of NT-SVOCg:
1 x 10-8
1 x 10-7
1 x 10-6
1 x 10-5
1 x 10-4
1 x 10-3
1 x 10-2
1 x 10-1
1
1 x 101
1 x 102
1 x 103
1 x 104
1 x 105
0
10
20
30
40
50
12:00 AM
4/10/2003
12:00 PM
12:00 AM
4/11/2003
12:00 PM
12:00 AM
4/12/2003
12:00 PM

Figure SI-21

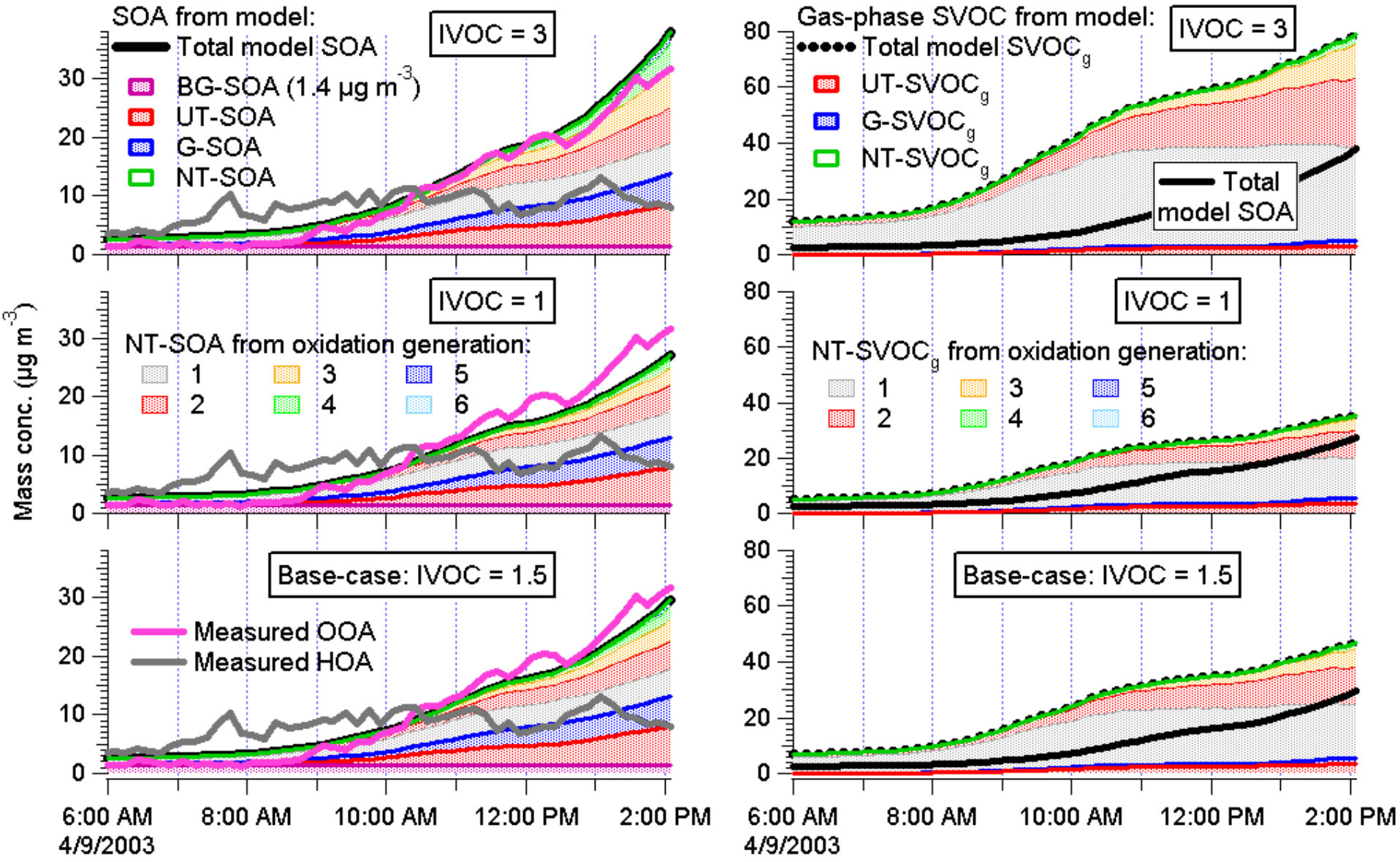
SOA from model:
Total model SOA
BG-SOA (1.4 µg m-3)
UT-SOA
G-SOA
NT-SOA
IVOC = 3
IVOC = 1
NT-SOA from oxidation generation:
1
2
3
4
5
6
Base-case: IVOC = 1.5
Measured OOA
Measured HOA
Mass conc. (µg m-3)
Gas-phase SVOC from model:
Total model SVOCg
UT-SVOCg
G-SVOCg
NT-SVOCg
Total model SOA
NT-SVOCg from oxidation generation:
6:00 AM
8:00 AM
10:00 AM
12:00 PM
2:00 PM
4/9/2003

Figure SI-22

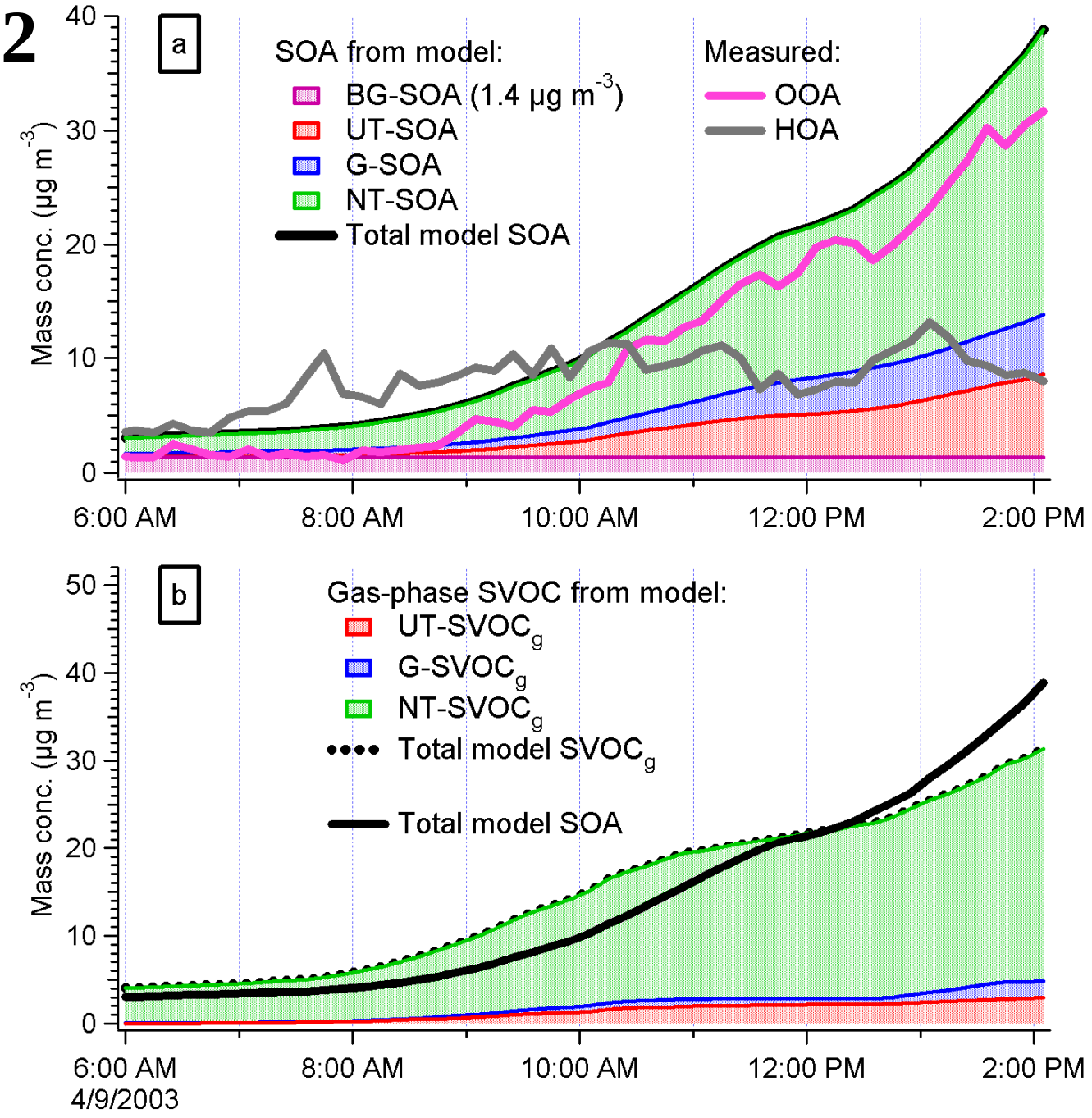
a
SOA from model:
BG-SOA (1.4 μg m-3)
UT-SOA
G-SOA
NT-SOA
Total model SOA
Measured:
OOA
HOA
Mass conc. (μg m-3)
0
10
20
30
40
6:00 AM
8:00 AM
10:00 AM
12:00 PM
2:00 PM
b
Gas-phase SVOC from model:
UT-SVOCg
G-SVOCg
NT-SVOCg
Total model SVOCg
Total model SOA
Mass conc. (μg m-3)
0
10
20
30
40
50
6:00 AM
4/9/2003
8:00 AM
10:00 AM
12:00 PM
2:00 PM

Figure SI-23

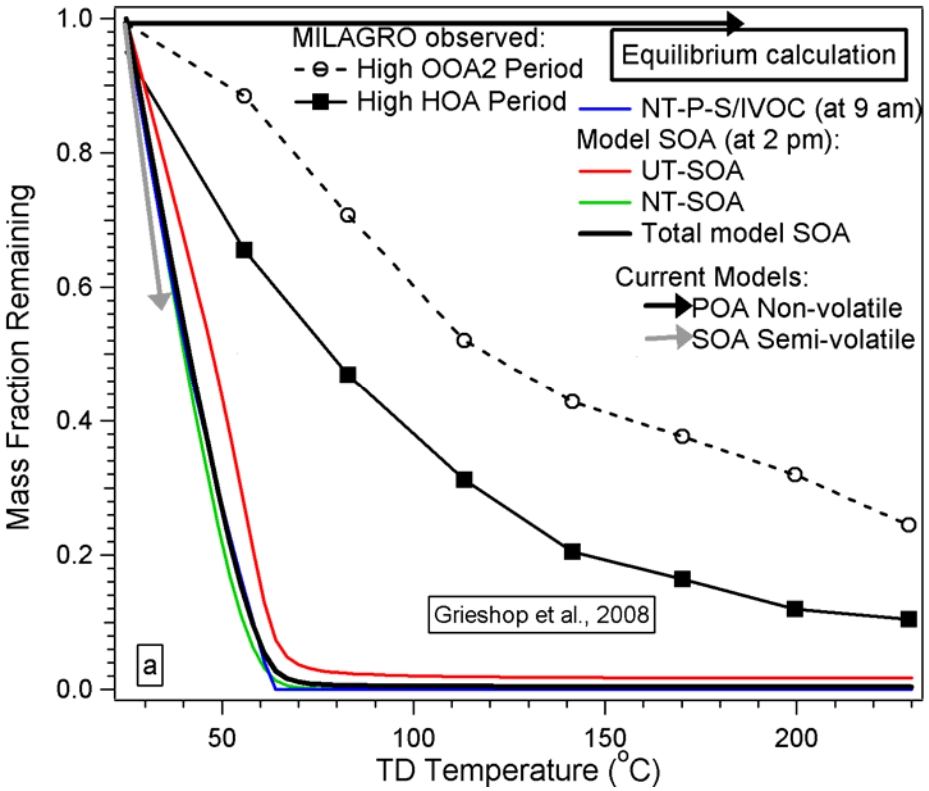
Mass Fraction Remaining
1.0
0.8
0.6
0.4
0.2
0.0
50
100
150
200
TD Temperature (°C)
MILAGRO observed:
High OOA2 Period
High HOA Period
Equilibrium calculation
NT-P-S/IVOC (at 9 am)
Model SOA (at 2 pm):
UT-SOA
NT-SOA
Total model SOA
Current Models:
POA Non-volatile
SOA Semi-volatile
Grieshop et al., 2008
a

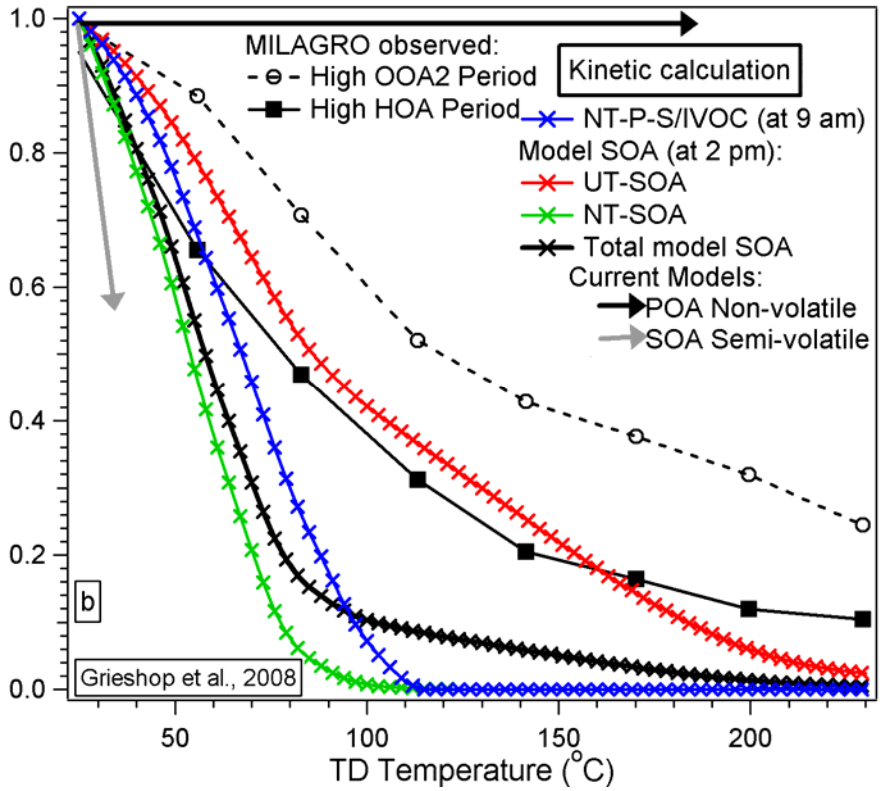
1.0
0.8
0.6
0.4
0.2
0.0
50
100
150
200
TD Temperature (°C)
MILAGRO observed:
High OOA2 Period
High HOA Period
Kinetic calculation
NT-P-S/IVOC (at 9 am)
Model SOA (at 2 pm):
UT-SOA
NT-SOA
Total model SOA
Current Models:
POA Non-volatile
SOA Semi-volatile
Grieshop et al., 2008
b

Figure SI-24

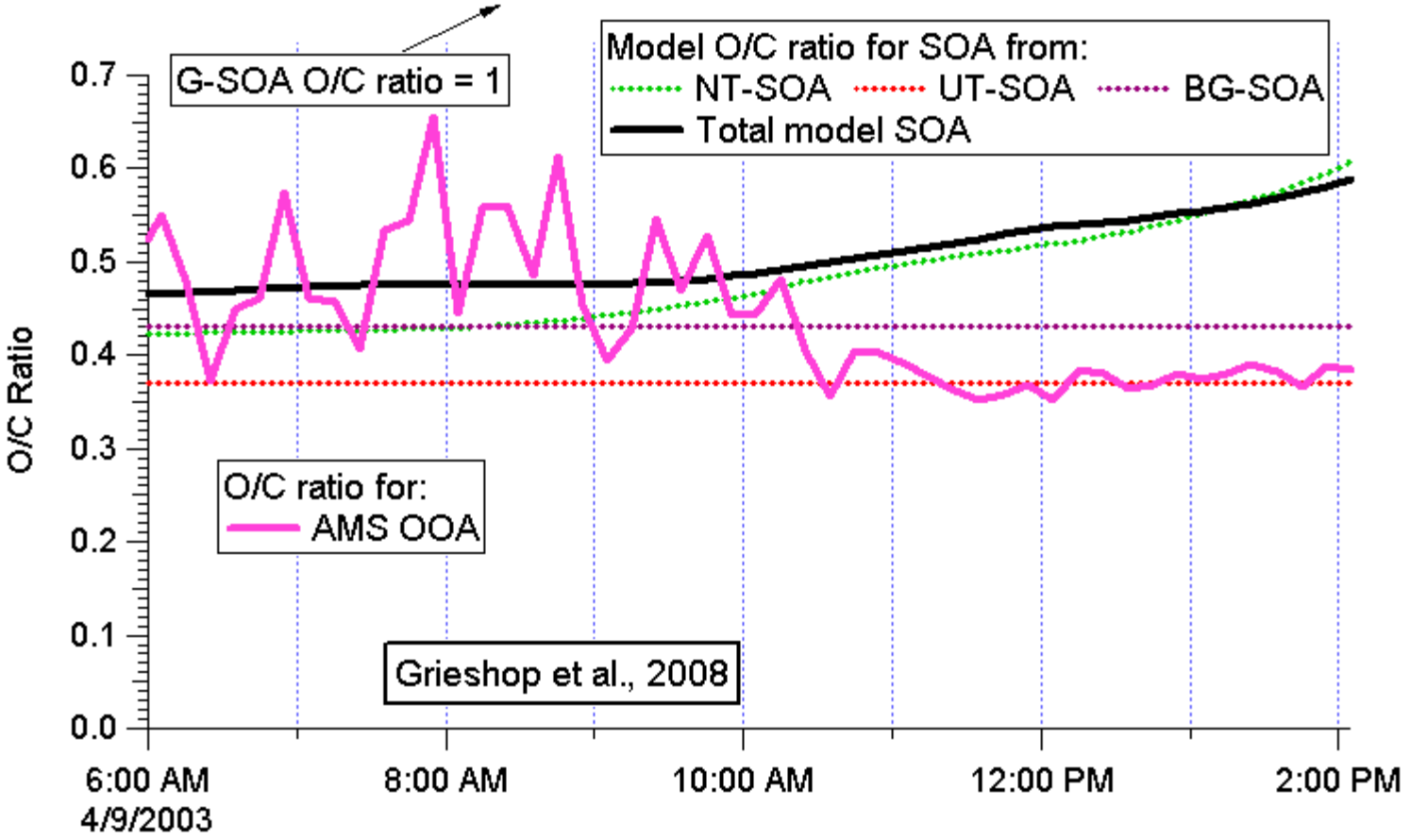
G-SOA O/C ratio = 1
Model O/C ratio for SOA from:
NT-SOA
UT-SOA
BG-SOA
Total model SOA
O/C ratio for:
AMS OOA
Grieshop et al., 2008
O/C Ratio
0.0
0.1
0.2
0.3
0.4
0.5
0.6
0.7
6:00 AM
4/9/2003
8:00 AM
10:00 AM
12:00 PM
2:00 PM

Figure SI-25

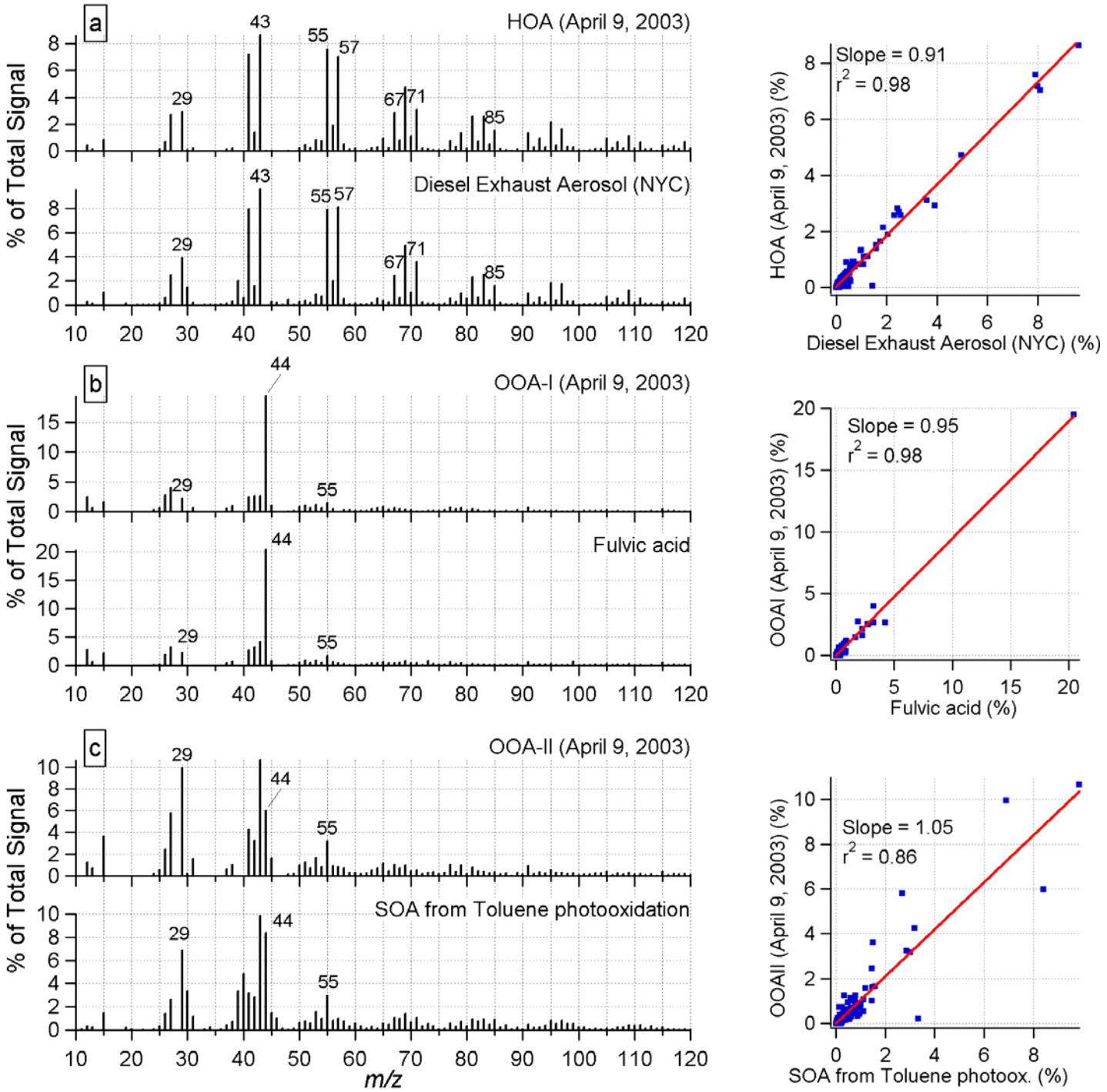
a
HOA (April 9, 2003)
Diesel Exhaust Aerosol (NYC)
% of Total Signal
b
OOA-I (April 9, 2003)
Fulvic acid
c
OOA-II (April 9, 2003)
SOA from Toluene photooxidation
m/z
Slope = 0.91
r2 = 0.98
HOA (April 9, 2003) (%)
Diesel Exhaust Aerosol (NYC) (%)
Slope = 0.95
r2 = 0.98
OOAI (April 9, 2003) (%)
Fulvic acid (%)
Slope = 1.05
r2 = 0.86
OOAII (April 9, 2003) (%)
SOA from Toluene photoox. (%)

Figure SI-26

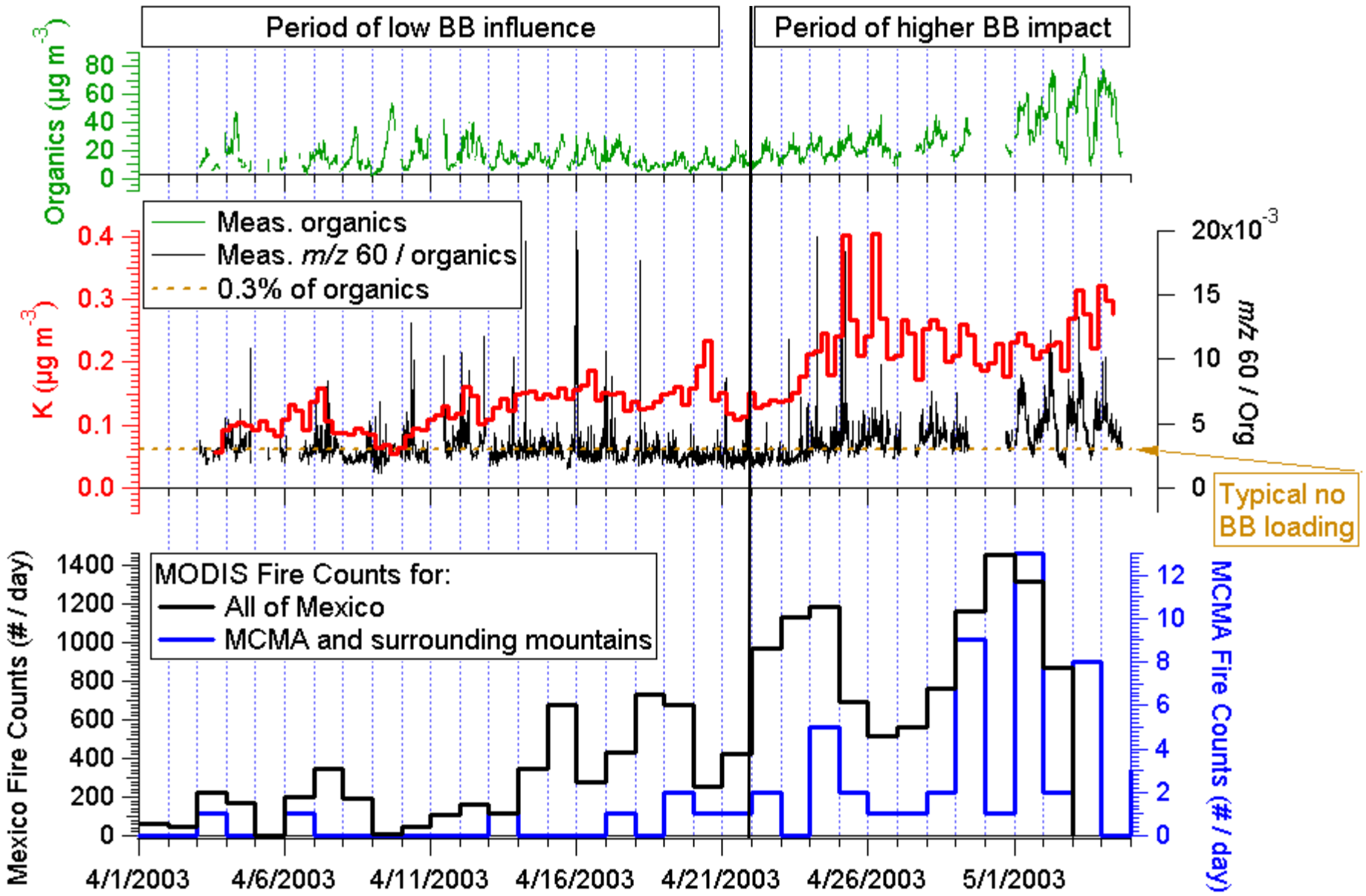
Period of low BB influence
Period of higher BB impact
Organics (µg m-3)
80
60
40
20
0
Meas. organics
Meas. m/z 60 / organics
0.3% of organics
K (µg m-3)
0.4
0.3
0.2
0.1
0.0
20x10-3
15
10
5
0
m/z 60 / Org
Typical no BB loading
MODIS Fire Counts for:
All of Mexico
MCMA and surrounding mountains
Mexico Fire Counts (# / day)
1400
1200
1000
800
600
400
200
0
12
10
8
6
4
2
0
MCMA Fire Counts (# / day)
4/1/2003
4/6/2003
4/11/2003
4/16/2003
4/21/2003
4/26/2003
5/1/2003

Figure SI-27

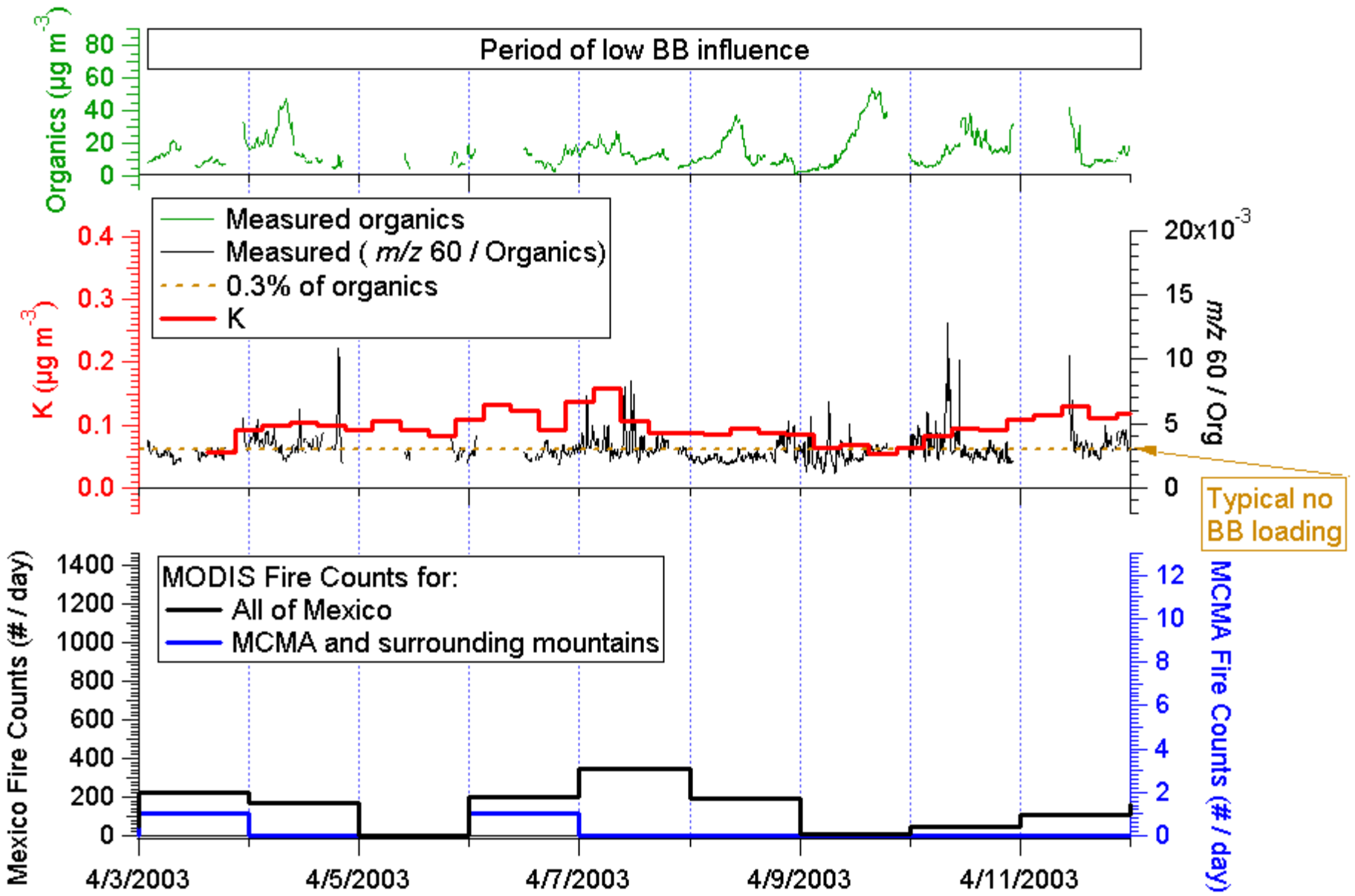
Organics (µg m-3)
80
60
40
20
0
Period of low BB influence
Measured organics
Measured (m/z 60 / Organics)
0.3% of organics
K
K (µg m-3)
0.4
0.3
0.2
0.1
0.0
20x10-3
15
10
5
0
m/z 60 / Org
Typical no BB loading
MODIS Fire Counts for:
All of Mexico
MCMA and surrounding mountains
Mexico Fire Counts (# / day)
1400
1200
1000
800
600
400
200
0
12
10
8
6
4
2
0
MCMA Fire Counts (# / day)
4/3/2003
4/5/2003
4/7/2003
4/9/2003
4/11/2003